Award Number: W81XWH-12-1-0127

TITLE: Altering the Microenvironment to Promote Dormancy of Metastatic Breast Cancer Cell in a 3D Bone Culture System

PRINCIPAL INVESTIGATOR:
Andrea M. Mastro

CONTRACTING ORGANIZATION: Pennsylvania State University
University Park, PA 16802-1505

REPORT DATE: April 2015

TYPE OF REPORT: Annual

PREPARED FOR: U.S. Army Medical Research and Materiel Command
Fort Detrick, Maryland 21702-5012

REPORT DOCUMENTATION PAGE

Form Approved
OMB No. 0704-0188

1. REPORT DATE	2. REPORT TYPE	3. DATES COVERED
April 2015	Annual	1 April 2014 - 31 March 2015

4. TITLE AND SUBTITLE

Altering the Microenvironment to Promote Dormancy of Metastatic Breast Cancer Cell in a 3D Bone Culture System

5a. CONTRACT NUMBER

5b. GRANT NUMBER
W81XWH-12-1-0127

5c. PROGRAM ELEMENT NUMBER

6. AUTHOR(S)

Andrea M Mastro and Erwin Vogler
email: a36@psu.edu

5d. PROJECT NUMBER

5e. TASK NUMBER

5f. WORK UNIT NUMBER

7. PERFORMING ORGANIZATION NAME(S) AND ADDRESS(ES)
Pennsylvania State University
University Park, PA 16802

8. PERFORMING ORGANIZATION REPORT NUMBER

9. SPONSORING / MONITORING AGENCY NAME(S) AND ADDRESS(ES)
U.S. Army Medical Research and Materiel Command
Fort Detrick, Maryland 21702-5012

10. SPONSOR/MONITOR'S ACRONYM(S)

11. SPONSOR/MONITOR'S REPORT NUMBER(S)

12. DISTRIBUTION / AVAILABILITY STATEMENT
Approved for Public Release; Distribution Unlimited

13. SUPPLEMENTARY NOTES

14. ABSTRACT Hypothesis: extracellular matrix (ECM) and bone microenvironment cytokines are critical for metastatic breast cancer cells to grow or remain dormant. This hypothesis is being tested using a 3D bioreactor of ECM, derived from osteoblasts (OB). Aim 1: determine how modification of the composition and structure of the ECM affects proliferation and dormancy. 1a. deprive OB of estrogen; 1b. stress the ECM; 1c. degrade the ECM with osteoclasts. Aim 2. determine how bone-remodeling and inflammatory cytokines affect proliferation and dormancy. 2a. add/block bone remodeling cytokines, 2b. add/block OB inflammatory stress response cytokines. The remodeling but not inflammatory cytokines permit dormant human cells to proliferate in the bioreactor in co-culture with OB. Proliferation depended on prostaglandin, (PGE2) production. Chronic oxidative stress of the ECM with H_2O_2 did not affect cancer cell growth. Howver estrogen deprivation or blocking the estrogen receptor permitted the dormant cells to proliferate. Human breast cancer cells grew better on decellurized matrix or on fixed osteoblasts than on intact matrix indicating that OB produce factor(s) antagonistic to cancer cells.

15. SUBJECT TERMS
Bone metastasis, 3D model, osteoblasts, cytokines, extracellular matrix

16. SECURITY CLASSIFICATION OF:	17. LIMITATION OF ABSTRACT	18. NUMBER OF PAGES	19a. NAME OF RESPONSIBLE PERSON
			USAMRMC

a. REPORT	b. ABSTRACT	c. THIS PAGE			19b. TELEPHONE NUMBER *(include area code)*
U	U	U	UU	42	

Table of Contents

Introduction

Breast cancer often metastasizes to the skeleton. The microenvironment of the bone plays an important role in determining whether the cancer cells grow or become dormant. We hypothesize that the extracellular matrix (ECM) and cytokines of the bone microenvironment are critical in determining the fate of the cancer cells. The study is being carried out in a relevant and innovative 3D model of bone-like tissue derived from osteoblasts. The aims are to determine how modification of the composition and structure of the ECM, and how cytokines and growth factors affect the cancer cells. The composition and structure of the ECM will be modified by deprivation of estrogen, oxidative stress, and by osteoclasts. Cytokines associated with bone remodeling and with inflammation will be added or blocked. We propose to use human primary osteoblasts with human MDA-MB-231 metastatic cells and their metastasis suppressed counterparts, MDA-MB-231BRMS1, and mouse MC3T3-E1 osteoblasts and murine mammary tumor cells D2A1(metastatic) or D2.OR(dormant).

Keywords: metastasis, bone, dormancy, matrix, cytokines, 3D model, estrogen, bone remodeling

Body

Hypothesis: The ECM and cytokines of the bone microenvironment are critical in determining whether metastatic breast cancer cells will grow or become dormant.

Specific aim: 1: To determine how modification of the ECM composition and structure affects proliferation and dormancy of breast cancer cells

Task 1 a. Deprive osteoblasts of estrogen

Osteoblasts express estrogen receptors. Estrogen is critical for osteoblast development of ECM. Furthermore, breast cancer occurs more commonly in postmenopausal women when estrogen is low. Thus, we asked if estrogen withdrawal during osteoblast differentiation would affect the growth of the cancer cells. In order to determine how an ECM formed under estrogen deprivation would affect the growth of cancer cells, murine osteoblasts, MC3T3-E1, were grown for 2 months in the bioreactor with a basal medium of αMEM with 10mM β-glycerophosphate and 50 μg/ml ascorbic acid. Normal FBS (N-FBS) was added in the growth chamber at a concentration of 10% to the control cultures. To simulate estrogen deprivation, 1μm of pure anti-estrogen ICI 182,780 was added to block the effect of estrogen contained in the N-FBS. Other cultures were deprived of estrogen by the use of 10% charcoal stripped FBS (CS-FBS) in place of the normal serum. In a subset of these cultures, 17β estradiol was added at 100pg/ml. We had found (reported in the previous progress report) that low estrogen in the cultures did not affect osteoblast differentiation, i.e. alkaline phosphatase production, but did suppress mineralization (von Kossa stain). Dormant/proliferating cancer cells were added at 2000 cells/cm^2 . Cultures were imaged by confocal microscopy. Proliferation was quantified with Image J analysis (Figure 1).

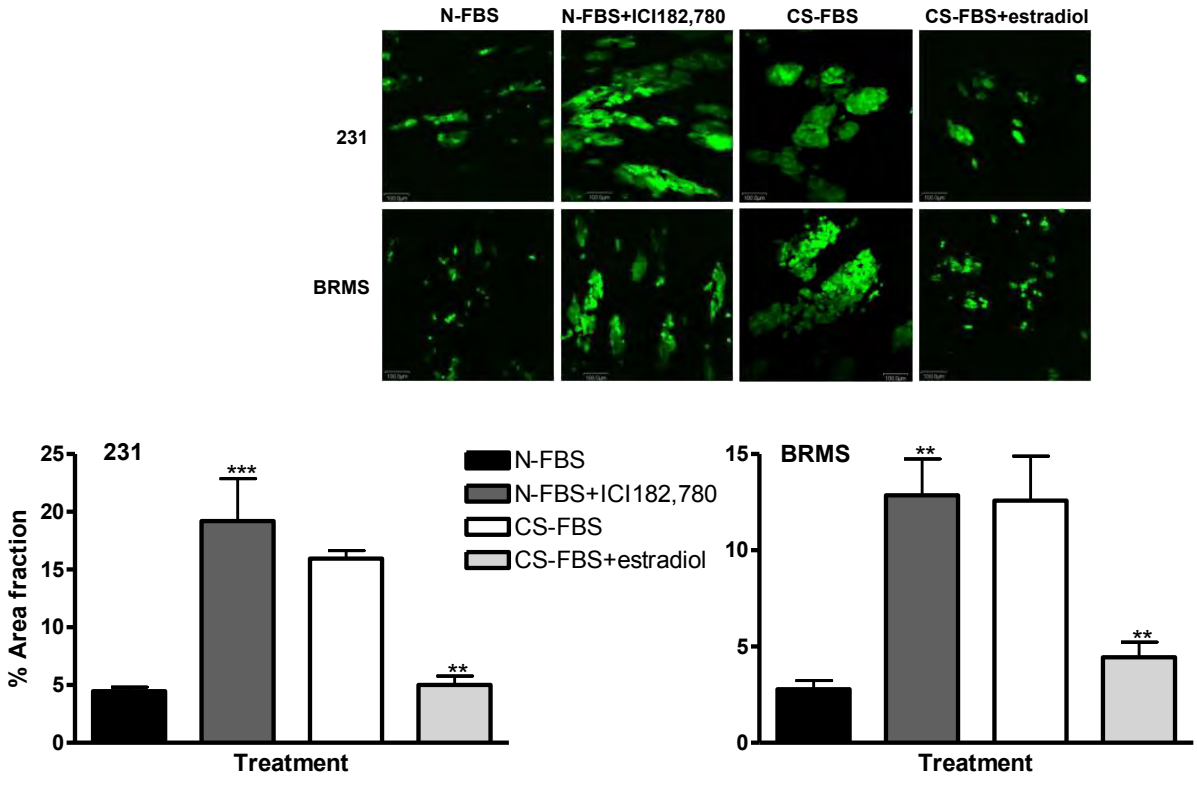

Figure 1. **Estrogen deprivation increased the growth and changed the morphology of MD-MB-231 and MDA-MB-231BRMS1 cancer cells.** Osteoblasts were cultured for two months in αMEM with 10mM β-glycerophosphate and 50 μg/ml ascorbic acid and 10% normal (N) FBS with and without the estrogen receptor antagonist, ICI182,780 (1μM). Osteoblasts were also cultured in the same medium with charcoal stripped (CS) FBS with and without 17-β estradiol (100pg/mL). GFP-expressing metastatic MDA-MB-231 or metastasis suppressed MDA-MB-231BRMS1 cancer cells, were added to each culture; estrogen conditions were maintained after addition of cancer cells. Images were collected daily for 5 days. Shown are representative images and quantitative data from day 5 (n=3). In both 231 and BRMS cells, growth increase occurred with lowered estrogen, i.e. addition of ICI182,780 or with the use of charcoal stripped serum. In cultures containing supplemental estradiol with CS-FBS, the growth and morphology reverted back to normal. Note that both cancer cell lines are estrogen receptor negative. **p<0.05; ***p<0.001

We found that estrogen deprivation of the osteoblast during the time they differentiated, led to an ECM that enhanced the growth of both metastatic and metastasis suppressed, ER negative, breast cancer cells. It is also known that estrogen suppresses inflammation in the bone. Although we have not yet tested for cytokines, we hypothesize that the breast cancer-osteoblast inflammatory response may be exacerbated with diminished estrogen (Carlsten, 2005).

Task 1. A. Assay in tissue culture

We asked if the same effects of estrogen manipulation could be detected on the matrix of osteoblasts grown in tissue culture plastic or in tissue culture glass chamber slides. This approach would permit us to work with more samples and with more manipulations than with the bioreactor. Moreover, it would permit us to collect preliminary data.

a.1 Differentiation and matrix mineralization

MC3T3-E1 osteoblasts were grown and differentiated in 24-well plates for 4 weeks, plus or minus 1 mM ICI. After 4 weeks, cultures were fixed and stained for alkaline phosphatase or prepared for von Kossa stain, the former an indicator of differentiation and the later and indicator of mineralization (Figure 2).

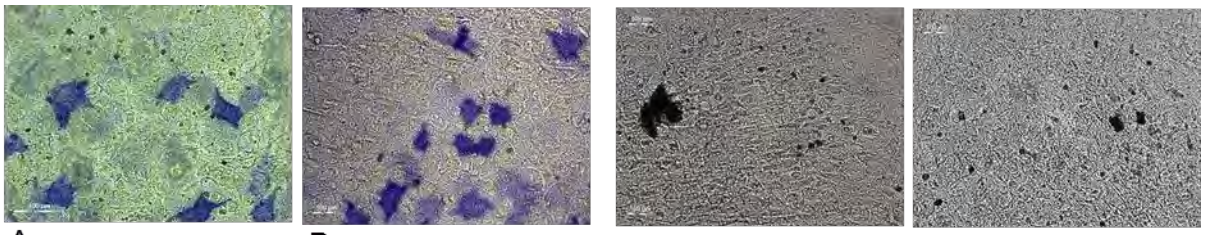

Figure 2. Blocking estrogen did not inhibit the expression of alkaline phosphatase or mineralization in cultures of MC3T3-E1. Osteoblasts were differentiated in a 24-well plate for 4 weeks in normal medium (A,C) or medium with ICI 182,780 an estrogen rececptor antagonist (B,D) before fixation and staining for alkaline phosphatase expression (A,B),or for mineralization (vonKossa stain, C,D). The substrate of the alkaline phosphatase enzyme, a marker of cell differentiation, stains a blue-purple color. Calcium mineralization is shown by the black specks (C,D). Light microscope images were taken after allowing the stain to dry. Scale bar = 100 μm.

a.2 Collagenous and non-collagenous proteins

We tested whether estrogen in the medium affected the collagenous and non-collagenous proteins produced by the osteoblasts (Figure 3). Compared to the matrix produced under normal growth condions (52pg/ml estradiol), the matrix produced in the presence of ICI had much less sirius red stain for collagen (Figure 3, A, B).

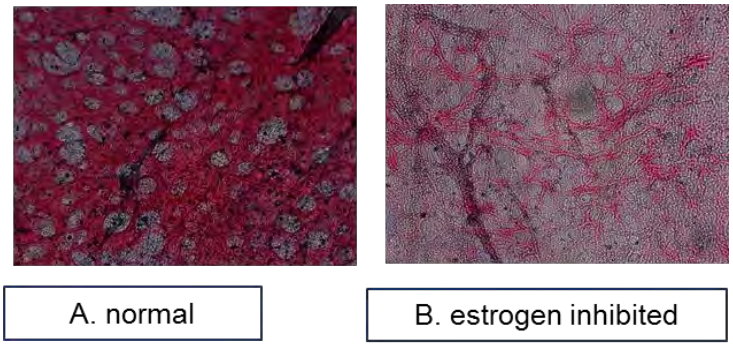

A. normal

B. estrogen inhibited

Figure 3. **Four-week control osteoblast matrix stained with Sirius red/ fast green (Chondrex).** Osteoblasts were differentiated in a 24-well plate for 4 weeks in normal media (A) or ICI medium (B) before decellularization of the matrix and staining with Sirius Red/Fast Green (Chondrex) for collagenous and non-collagenous proteins, respectively. After washing away excess dye, samples were allowed to dry and were photographed using light microscopy (Right). In another set of experiments (Table 1,below) the bound dye was eluted and optical density at 540 nm and 605 nm was used to calculate the collagenous and non-collagenous proteins, respectively. Samples were taken at 3 weeks and 4 weeks of growth.

Table 1. Collagenous and non-collagenous proteins in matrices of ostetoblasts grown with supplemental estrogen or with ICI, an extrogen receptor antagonist.

	Total protein (ug)		Collagenous/non-collagenous	
	3 weeks	4 weeks	3 weeks	4 weeks
Normal matrix	49.2	50.2	0.22	0.26
Estrogen inhibited matrix (ICI)	30.5	32.3	0.18	0.17
Estrogen supplemented matrix (E2)	53.1	73.2	0.27	0.24

This loss of collagen was also detected when the dyes were eluted and quantified (Table 1). At three weeks the collagen produced in the presence of ICI was about 45% less than that seen with the cells grown under normal conditions. At 4 weeks the values remained about the same (42%). The non-collagenous proteins with ICI were about 37% of the values as the cells grown in normal medium. The values for the cultures supplemented with estradiol (252 pg/m/ total), were about 30-40% higher than that of the normal cultures,(52 pg/ml estradiol).

a.3 Matrix structure

We used the collagen-binding protein, CNA-35, to compare the general structure of the matrix of MC3T3-E1 osteoblasts grown with control, estrogen inhibited and estrogen supplemented media. The CNA-35 was labeled with Alexafluor 568. The images were compared (Figure 4).

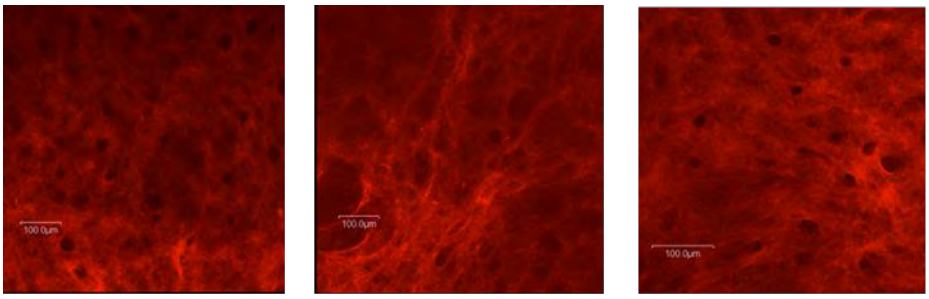

A. Control medium, 52 pg/ml estradiol

B. Medium with ICI 182,780

C Medium supplemented with estradiol, 200 pg/ml

Figure 4. Estrogen levels affected the matrix deposition by MC3T3 osteoblasts. The osteoblasts were grown in A. normal medium, 52 pg/ml estradiol, B. medium with ICI 182,780 receptor antagonist, and C. medium supplemented with 200 pg/ml estradiol for three weeks. The cultures were washed with PBS, fixed and imaged with confocal microscopy. They were not decellurized.

We added cancer cells to the various matrices after they had been decellurized (Figure 5). The most apparent change in overall matrix structure was the appearance of elongated fibrils in the matrix of the cells grown with the ICI (Figure 4, compare B with A and C).

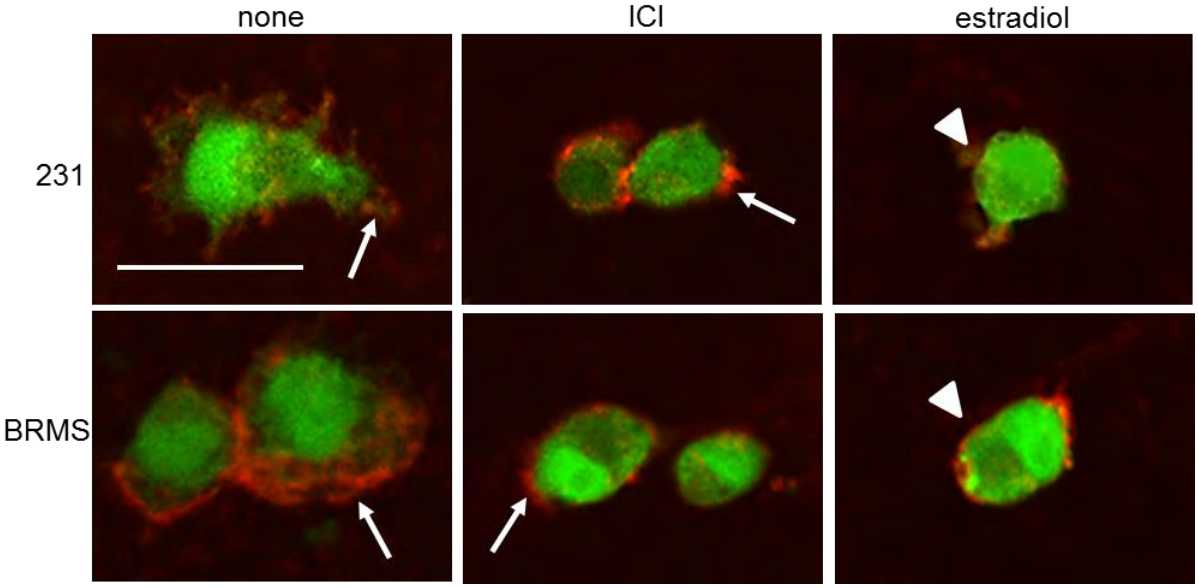

Figure 5. Estrogen status during bone matrix production altered actin fiber arrangement of breast cancer cells attached to a decellularized osteoblast matrix. MC3T3-E1 osteoblasts were grown for 3 weeks on chamber slides in differentiation media with no additives (52 pg/ml estradiol), or with 1μM ICI or with 252 pg/mL estradiol. Matrices were decellularized and seeded with either MDA-MB-231^{GFP} or MDA-MB-231BRMS1^{GFP} cells. After 6 hours, slides were rinsed and labeled with phalloidin conjugated to Alexa 568 (Life Technologies). Cells were imaged with an Olympus FV300 confocal microscope. Arrows note extended actin fiber structure in cells plated on unaltered or ICI matrices while cells plated on estradiol supplemented matrices maintain a ring-like formation (arrowheads). Scale bar = 50 microns.

Both MDA-MB-231 cells and the isologous line, the metastasis suppressed MDA-MB-231BRMS1, were examined for attachment after 6 hours with osteoblasts grown under the three estrogen conditions (Figure 5). The osteoblasts were first removed from the matrix decellularized with deoxycholate. The cells on matrix grown with 52 pg/ml estradiol, the normal matrix, show extended fiber structures (Figure 5 left). Under conditions of estradiol supplementation or blocking of estradiol with ICI, the cells did not shown this extended structure. These data support the previous finding (Figure 3,4) that the matrix has been altered and in such a manner that affects the cancer cells.

1.4 Attachment and Growth on a fixed vs live cell matrix

We carried out a series of experiments to determine how the matrix affected the attachment and growth of the breast cancer cells (Figure 6). We compared attachement and growth on tissue culture plastic to that on an osteoblast layer of live osteoblasts, fixed osteoblasts or a deoxycholate decellularized matrix.

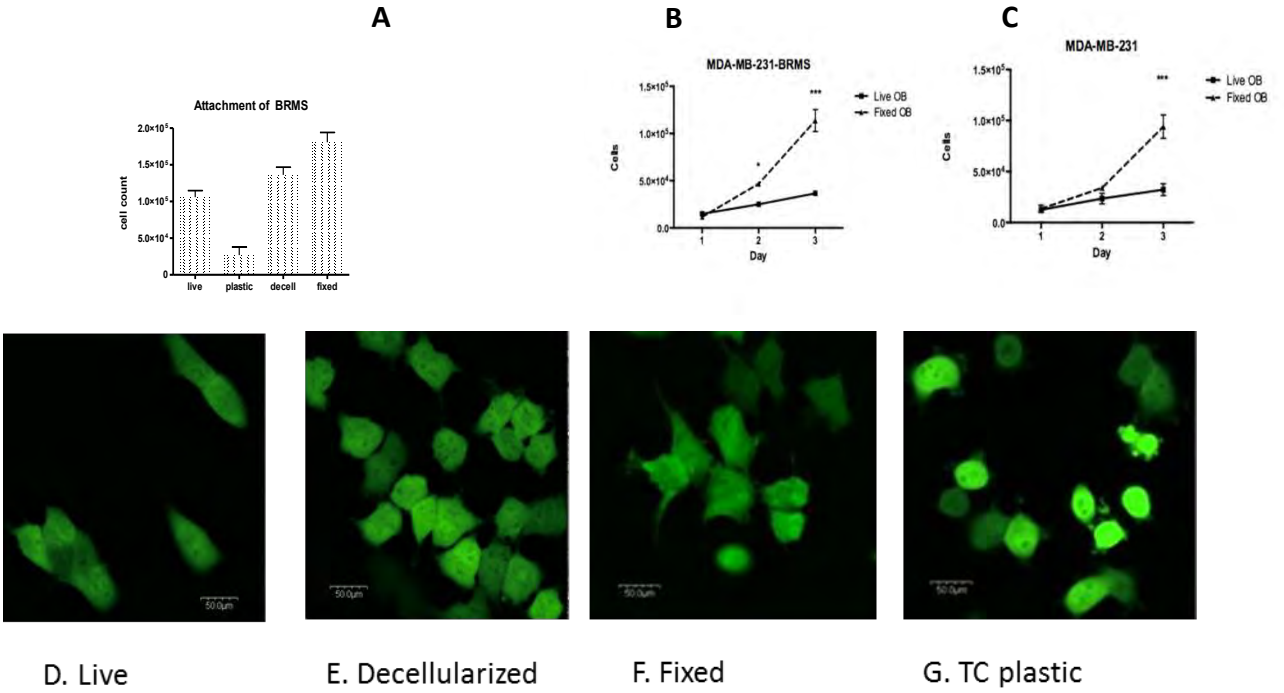

Figure 6. Breast cancer cells attached and grew better on a fixed osteoblast matrix. A. Attachment of MDA-MB-231BRMS1^{GFP} was determined after 6 hours of incubation on tissue culture plastic, a culture of live MC3T3-E1 osteoblasts of 3 weeks, a culture decellularized with deoxycholate, or a culture fixed with 4% paraformaldehyde. Cells were lysed and GFP in the lysate was determined. The growth of MDA-MB-231^{GFP} (B) or MDA-MB-231BRMS1^{GFP} (C) was determined on live cultures or fixed osteoblasts. N=3 for each assay. $P<0.001$. D-G Images of MDA-MB-231 cells on various matrices after 18 hours. Scale bar = 50 µM.

We found that with both cell lines (Figure 6), more cells attached to the osteoblasts matrix that had been fixed compared with the live osteoblasts. Ten-fold more attached than on tissue culture plastic. We compared the growth of the cancer cells over 3 days (Figure 6, B,C) and saw that the attachment was reflected in cell growth.

We speculated that osteoblasts were producing inhibitory materials of some kind. However, conditioned medium from osteoblasts added to cancer cells did not affect their attachment for growth. It may be that one of the inhibitors is formed when the cancer cells attach to the osteoblasts. We have published previously (Bussard et al., 2010) that the osteoblasts show an inflammatory response when in contact with the cancer cells. We imaged the cells grown on the various matrices (Figure 6, D-G). Compared to plastic, the cells on a matix were much more spread and flattened. On the live matrix of osteoblasts, the cancer cells remained in small colonies; while in the fixed cultures they tended to be more spread apart.

Task 1. b. Treat the ECM with H_2O_2 prior to the addition of cancer cells.

As reported in the 2013 progress report, we found no significant difference in breast cancer cell growth after treatment of the ECM with H_2O_2. We varied concentrations and times of addition but saw no changes in the cancer cell growth.

Task 1.c. Incubate the osteoblast tissue with osteoclasts to partially degrade the matrix.

Pre-osteoclasts must be isolated from the bone marrow and differentiated to active osteoclasts. We have had limited trials of addition of osteoclasts to the bioreactor. However, we were able to mimic aspects of bone remodeling in the bioreactor (Krishnan et al., 2014). Addition of cancer cells showed an affinity for the cancer cells with the osteoclasts.

Characterization of the collagen matrix

As described in our last progress report, we had submitted samples of cultures of MC3T3-E1 grown in the bioreactor for two months, to Dr. Patricia Keeley at the University of Wisconsin-Madison to characterize the collagen by second harmonica generation analysis (Gehler et al., 2013). Unfortunately she was unable to resolve the collagen to the desired degree of resolution for second harmonic generation studies. However, we had read of a novel and recently discovered collagen binding protein, CNA35, isolated from S. aureus, that could be labeled with a fluorescent probe (Zong et al., 2005). This molecule can be used with live or fixed cultures. We obtained CNA35 from Dr.Magnus Hooke, Texas A&M. We conjugated it with either Alexa Fluor 568 or 488. The conjugated protein was used in cultures at 0.05 μM. We were successful in labeling collagen fibrils in 2D and 3D cultures (Figure 7). MDA-MB-231 GFP expressing cancer cells were added to cultures of MC3T3-E1 at 4000 cells/cm^2. After 3 days of co-culture the cells were stained with CNA35-Alexa Fluor 568 and imaged by confocal microscopy. The collagen arrangements of the matrices were different for the same cells grown under the two different conditions (compare Figure 7A with Figure 7B).

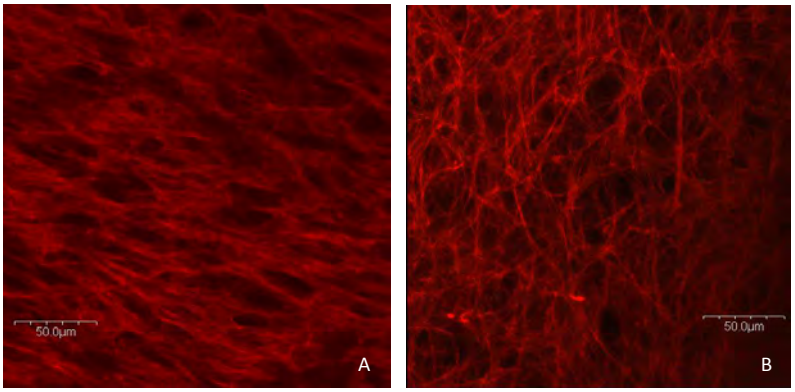

Figure 7. MC3T3-E1 osteoblast matrix labeled with CNA35-Alexafluor 568 in 2D (A) or 3D (B) cultures. MC3T3-E1 were cultured in tissue culture plastic plates (A) for 3 weeks or in the bioreactor (B) for 4 weeks with αMEM, 1% β-glycerol phosphate and 50 µg/ml ascorbic acid. CNA35 was added to fixed cultures at 0.05 µM. Images were taken with confocal microscopy. Scale bar = 50µM.

GFP-expressing MDA-MB-231 cells were added to 2D cultures and imaged 3 days later (Figure 8). The cancer cells aligned themselves within and along the matrix and appeared to remodel the neighboring fibers.

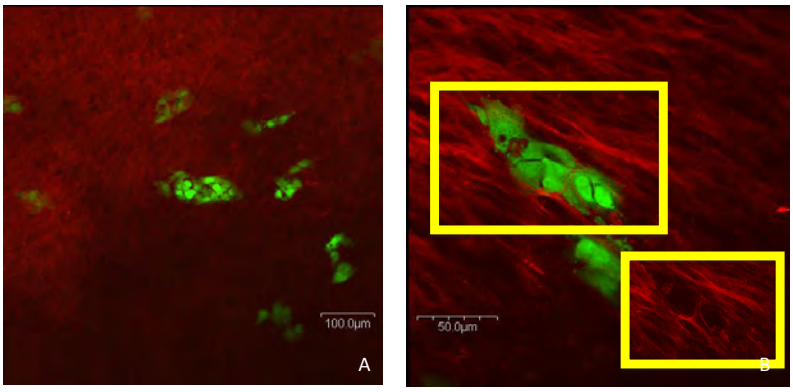

Figure 8. Remodeling of osteoblast-produced ECM by MDA-MB-231 cells in 2D cultures. MC3T3-E1 osteoblasts were cultured for 3 weeks before addition of MDA-MB-231-GFP (4000 cells/cm^2). Three days later the cultures were fixed, stained and imaged with confocal microscopy. A, 20X; B, 60X magnification. Note the changes in the ECM close to the cancer cells, and that some cancer cells are buried in the ECM. Scale bar = 50µM

We also tested the MDA-MB-231-GFP cells in the bioreactor (Figure 9). The MC3T3-E1 had been grown for 4 weeks prior to the addition of cancer cells. They were imaged as in Figure 8 . The matrix in the bioreactor appears to be thicker than in the culture dish. Thus it is more difficult to see the changes in the individual collagen fibers.

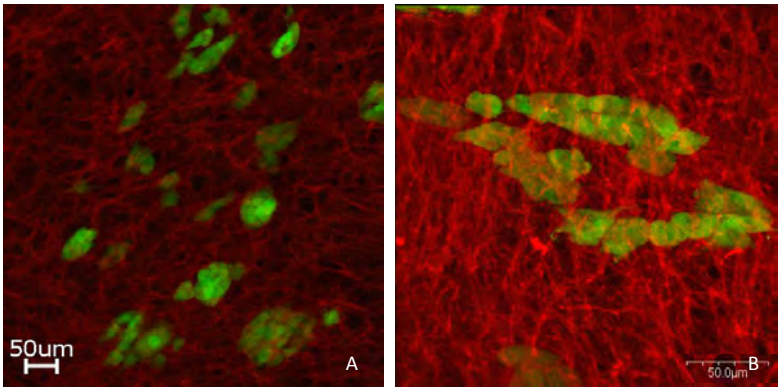

Figure 9. Metastatic MDA-MB-231 cells invaded the ECM in the bioreactor. The cancer cells were added to 4 week cultures of MC3T3-E1 cells. After 3 days the cultures were fixed, stained with CNA35 conjugated to Alexa Fluor 568 and imaged with confocal microscopy at 20X (A) or 60X (B). Note how the cancer cells are imbedded beneath the matrix. Scale bar = 50µM

In another set of bioreactor cultures we tested the metastasis suppressed variant of MDA-MB-231, MDA-MB-231-BRMS1 cells (Figure 10).

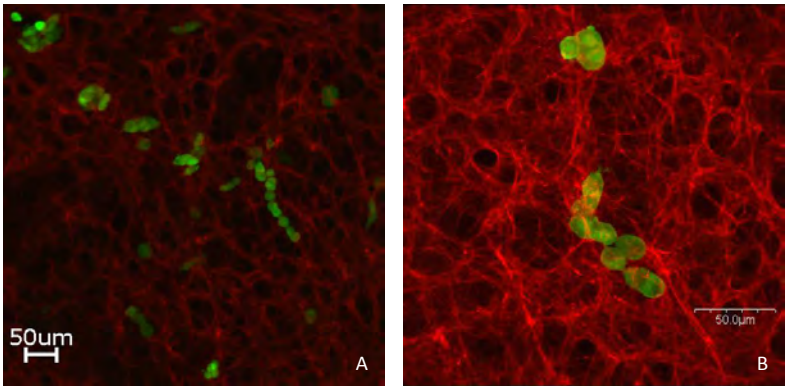

Figure 10. MDA-MB-231BRMS1 cells were less invasive in the ECM. MC3T3-E1 cells were grown in the bioreactor for 4 weeks before the addition of the metastasis suppressed cancer cells. After 3 days the cultures were fixed, stained with CNA35 Alexa-568 and imaged with confocal microscopy at 20X (A) or 60X (B). In comparison to the metastatic MDA-MB-231 cells the BRMS cells remained above the matrix. Scale bar = 50µM

The CNA35 has provided us a tool to begin to investigate the interaction of the cancer cells with the ECM and to ask how the ECM affects the growth of the cancer cells. We used the CNA35 to examine the matrix after deprivation of estrogen (Figure 4).

Atomic Force Microscopy

Atomic force microscopy will provide a wealth of information to characterize the bone-like matrix. The Bruker ICON located in the Materials Research Institute, Penn State University Park, is capable of performing peak force tapping analysis which is particularly well suited for atomic force microscopy of delicate biological samples. The instrument has expanded capability to acquire quantitative information for such matrix characteristics as topography, elasticity, stiffness and adhesion. A member of our research team has attended a two day workshop on the principles and operation of the atomic force instrumentation. We plan to characterize and compare samples of the native-made osteoblast matrix with and without cancer cells.

Specific Aim 2: **To determine how bone remodeling and inflammatory cytokines in the microenvironment affect proliferation and dormancy of cancer cells**.

This work has recently been published (see appended publication, Sosnoski, DM, RJ Norgard, CD Grove, SJ Foster and Andrea M. Mastro, Dormancy and growth of metastatic breast cancer cells in a bone-like microenvironment. Clin Exp Metastasis, 32: 335-344, 2015). The findings are briefly summarized here.

Task 2a: Cocktails of cytokines associated with bone remodeling were tested for the effects on growth/dormancy of cancer cells.

Bioreactor MC3T3-E1/Human Breast Cancer Cell Model

In the 2013 progress report, we reported that MDA-MB-231BRMS1 breast cancer cells entered a dormant state when cultured in a bioreactor with differentiated MC3T3-E1 murine osteoblasts. The osteoblasts at two months of culture had formed a thick collagen matrix (Mastro and Vogler, 2009). We tested various combinations of inflammatory and bone remodeling cytokines to determine if they could release the BRMS cells from the dormant state. The cocktail of inflammatory cytokines (IL-6, MCP-1, IL-8, VEGF and GRO-α) was not effective. However when a cocktail of bone remodeling cytokines (TNFα, IL-1β and IL-6) were added, the cells proliferated and exhibited a dramatic change in morphology (Figure 11 and see Figure 1 in appended publication). To demonstrate that the cytokines were directly responsible shift to the proliferative state, we

carried out experiments in which the cytokines were inhibited by neutralizing antibodies. MC3T3-E1 cells were grown and differentiated in the bioreactor for two months, establishing a mature osteoblast population with a native collagenous matrix. The human breast cancer cell lines were added (4000 cells/cm^2) to the bottom chamber of the bioreactor cultures; 15 minutes later, a limited panel of bone remodeling cytokines (TNFα (5ng/mL), IL-1β (10ng/mL), and IL-6 (10ng/mL)) was added. Neutralizing antibodies to each of the cytokines were added to the cytokine cocktail in 600-2000 fold excess. Cytokines and antibodies were purchased from R&D Systems, Minneapolis, MN. Cultures were photographed daily by confocal microscopy for morphological and proliferative changes in the cancer cells. On the final day of culture, bioreactors were dismantled and the culture membranes fixed in 4% paraformaldehyde. Culture supernatants were frozen for later cytokine analysis. Image J analysis was conducted on collected confocal images to determine percent area fraction. Results are the average of 3 images collected at each time point. Statistical analysis was performed in GraphPad Prizm using 2-way ANOVA.

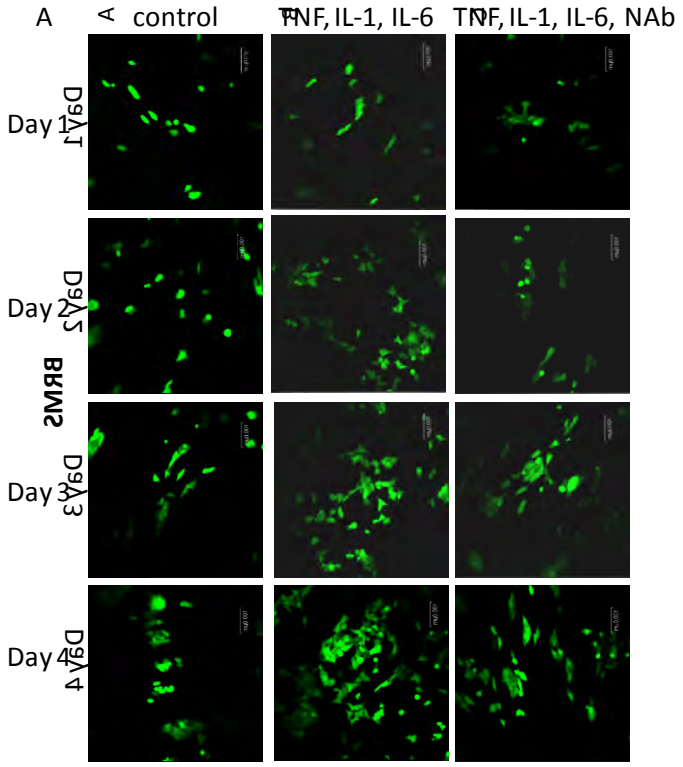

Figure 11. The effects of BRC on BRMS cells were mitigated by neutralizing antibodies. A) TNFα, IL-1β and IL-6 were added to the 3D osteoblast culture along with neutralizing antibodies. Cultures were imaged daily for 4 days. Shown are representative images for each time. B) Area fraction quantitation was performed on images (n=3) using ImageJ. **p<0.01 ; ***p<0.001

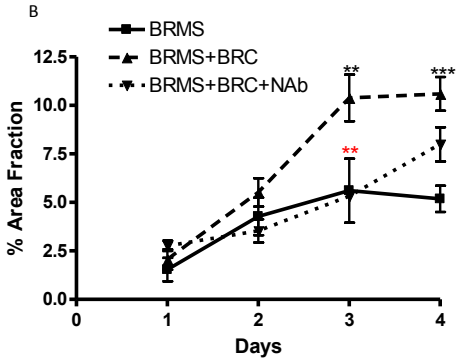

The presence of the neutralizing antibodies to the bone remodeling cytokines blocked the proliferative and morphological changes elicited in the MDA-MB-231BRMS1 cells (Figure 11 A). However, after three days in culture this effect diminished (Figure 11 B). It is possible that the antibodies were degraded to the point that they were no longer effective.

Next, we set out to investigate possible mechanisms for the "awakening" of the dormant BRMS1 cells by the bone remodeling cytokines. A search of scientific literature revealed a strong correlation between cyclooxygenase-2 (COX-2) and its downstream product, prostaglandin E2 (PGE) in the tumorgenesis and invasion of breast cancer cells (Mitchell et al., 2010). Cultures were established as previously described. The COX-2 inhibitor, indomethacin (Sigma-Aldrich, St. Louis, MO) was added to select cultures at a concentration of 50μM. Cultures were photographed daily by confocal microscopy for morphological and proliferative changes in the cancer cells. On the final day of culture, bioreactors were dismantled and the culture

membranes fixed in 4% paraformaldehyde. Culture supernatants were frozen for later cytokine analysis. Image J analysis was conducted on collected confocal images to determine percent area fraction. Results are the average of 3 images collected at each time point. Statistical analysis was performed in GraphPad Prizm using 2-way ANOVA.

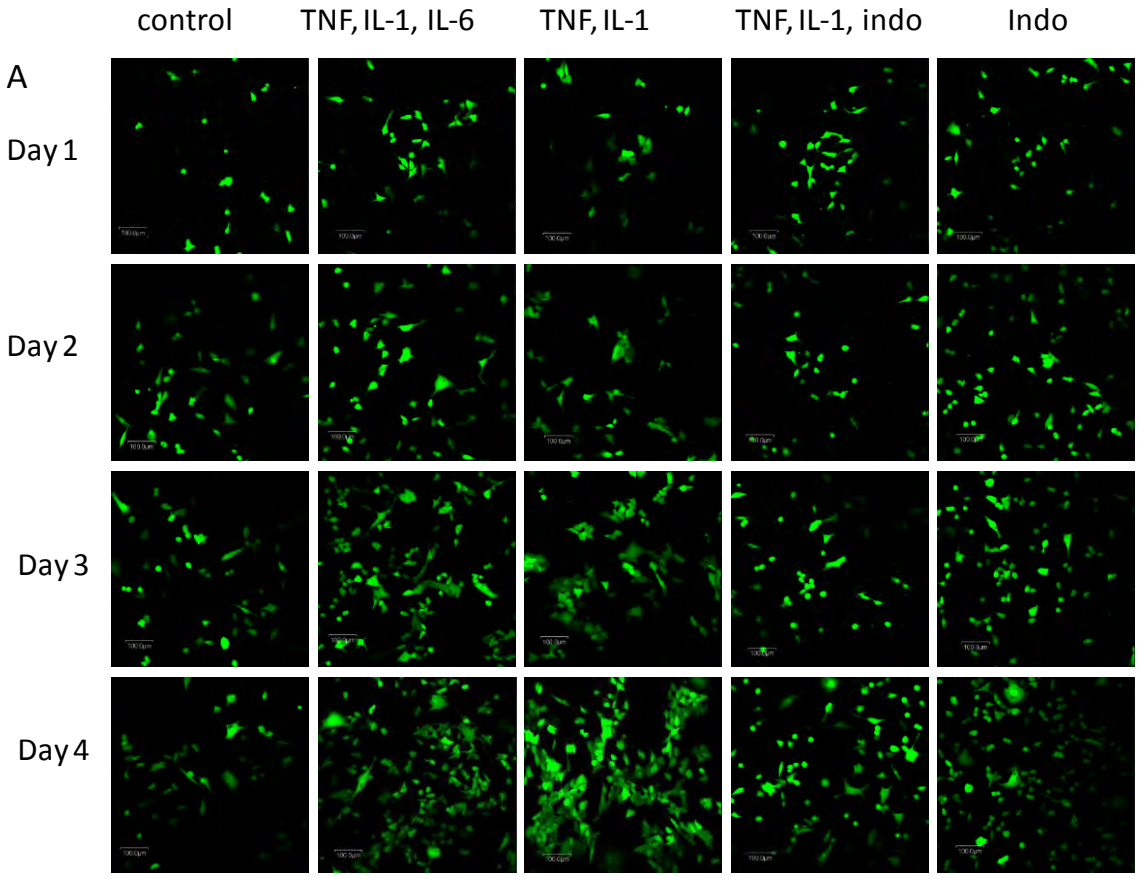

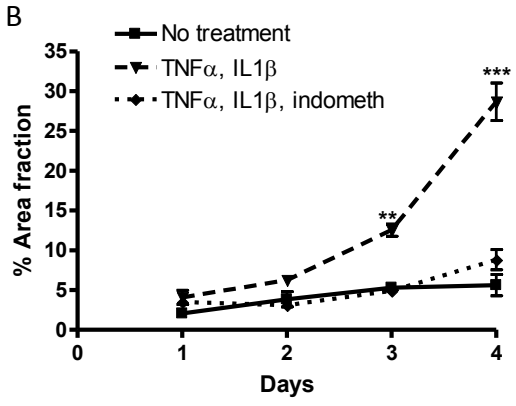

Figure 12. The effects of TNFα, IL-1β on MDA-MB-231 BRMS1 cells were blocked by indomethacin. A) TNFα, IL-1β and IL-6 were added to the 3D osteoblast culture. A TNFα and IL-1β cocktail was also tested along with 50μM indomethacin. Cultures were imaged daily for 4 days. B) Area fraction quantitation was performed on images (n=3) using ImageJ and GraphPad Prizm

From this experiment, we determined that IL-6 was not required for the BRMS1 cells to break dormancy; TNFα and IL-1β were sufficient to cause the proliferative and morphological changes. The addition of 50μM indomethacin caused the cells to maintain their dormant state, even in the presence of the bone remodeling cytokines (Figures 12A and 12B and Figure 2, appended publication) .

In light of these findings, we decided to target molecules downstream of COX-2 in the arachidonic acid cascade, namely PGE2. The prostaglandin receptor antagonist AH6809 (from Cayman Chemical, Ann Arbor, MI) was added to the cultures at a concentration of 50μM simultaneously with the TNFα and IL-1β. Cultures were maintained and images collected daily for 4 days.

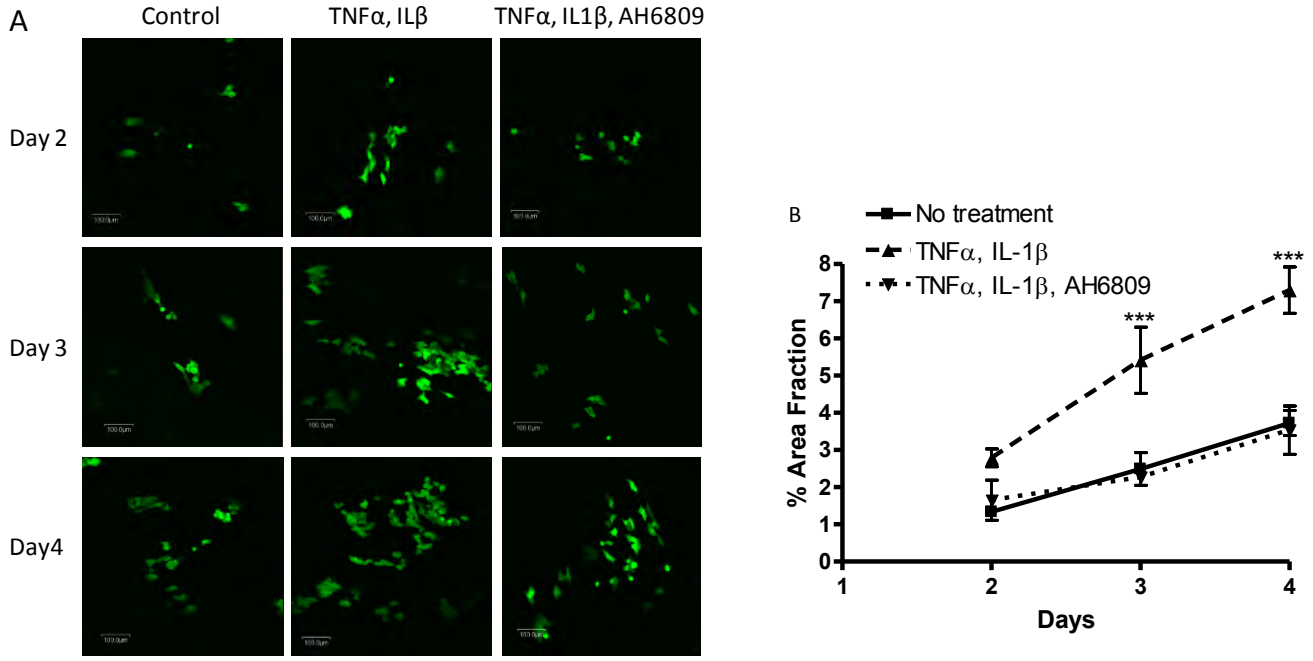

Figure 13. The effects of TNFα, IL-1β on MDA-MB-231BRMS1 cells were blocked by the PGE2 receptor antagonist, AH6809. TNFα and IL-1β were added to the 3D osteoblast culture along with 50μM AH6809. Cultures were imaged daily for 4 days. A) Representative images of live bioreactor cultures captured by confocal microscopy. B) Area fraction quantitation was performed on images (n=3) using ImageJ; graph and statistical analysis was performed on GraphPad Prizm using 2-way ANOVA. ***p<0.001

The prostaglandin receptor inhibitor AH6809 had a marked inhibitory effect on the proliferation and morphology changes induced by the bone remodeling cytokines TNFα and IL-1β (Figure 13A). The area fraction occupied by cancer cells was reduced to the same level as the co-culture without additional cytokines (Figure 13B). These data suggest that PGE2 plays a key role in the switch of a breast cancer cell from a dormant to an active state. In order to investigate this link, we assayed the reserved supernatants from the bioreactor cultures for levels of PGE2 using an EIA based kit (GE Healthcare, Piscataway, NJ). Assays were performed according to the manufacturer's protocol with recommended modifications to allow for the high protein content of the bioreactor supernatants.

Table 1 Production of PGE2 in bioreactor cultures of MDA-MB-231BRMS1 cells with MC3T3-E1

Treatment	PGE2 (pg/mL) ± SD
None	518 ± 2
TNFα, IL-1β	35,108 ± 115
TNFα, IL-1β, NAb	368 ± 171
TNFα, IL-1β, indo	379 ± 71
TNFα, IL-1β, AH6809	32,450 ± 2963
Untreated MC3T3-E1	522 ± 10

Table 1 from appended publication (Sosnoski et al 2015). PGE2 levels are elevated by the bone remodeling cytokines, but reduced by addition of indomethacin or neutralizing antibodies. The results of two separate experiments are summarized in the tables above. In both cases, PGE2 levels are elevated well above the level of untreated cultures while levels are decreased in cultures with added indomethacin or neutralizing antibodies. The PGE2 receptor inhibitor AH6809 did not lower the level of PGE2 induced by the bone remodeling cytokines.

The levels of PGE2 were substantially elevated when TNFα and IL-1β were present. That elevation was mitigated by the addition of the COX-2 inhibitor, indomethacin which prevented the downstream production of PGE2 in the arachidonic acid metabolic pathway. While the cultures containing the cytokines plus the PGE2 receptor inhibitor, AH6809 produced high levels of PGE2, the cytokine-associated effects on growth and morphology of the BRMS1 cells were halted by the inability of the prostaglandin to bind to the cell receptor. These data indicated that the bone remodeling cytokines TNFα and IL-1β caused dormant cells in a bone microenvironment to proliferate via increased production of prostaglandin E2 and its subsequent signaling.

We carried out immunohistochemistry to assay for nuclear localization of Ki67 as a marker for cell proliferation (Figure 14 ,Figure 3 in appended publication). About 2% of the cells showed nuclear localization of Ki67 in the untreated cultures. This value increased to 28% in the presence of TNFα and IL-1β or 24% with PGE2. With AH6809 no positive cells could be found (0%) (Figure 14).

Figure 14

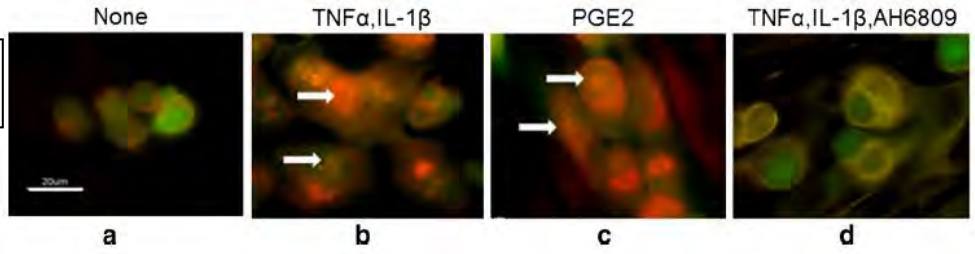

Fig. 3 Nuclear localization of the proliferation marker, Ki67, was increased in co-cultured BRMS1 cells exposed to TNFα and IL-1β or PGE2 Co-cultures were assembled and treated as described in the "methods" section. After 4 days, cultures were disassembled; segments of the culture membrane were fixed and stained by fluorescent immunocytochemistry for the presence of Ki67. Percentage of cells positive for Ki67 nuclear staining was determined from 50 cells per treatment group. Shown are images from **a** untreated culture (2 %) and cultures treated with **b** TNFα and IL-1β (28 %), **c** PGE2 (24 %) or **d** TNFα, IL-1β and PGE2 receptor inhibitor AH6809 (0 %). Positive nuclear staining is indicated by *arrows*. *Scale bar* 20 microns

We had also determined that the non- metastatic MCF-7 line became dormant when cultured on normal human osteoblasts in the bioreactor (Figure 15, Figure 4 from appended publication). The cytokines included reported human bone remodeling cytokines (Table a, below). The increase in proliferation was blocked with indomethacin or with AH6809.

Figure 15

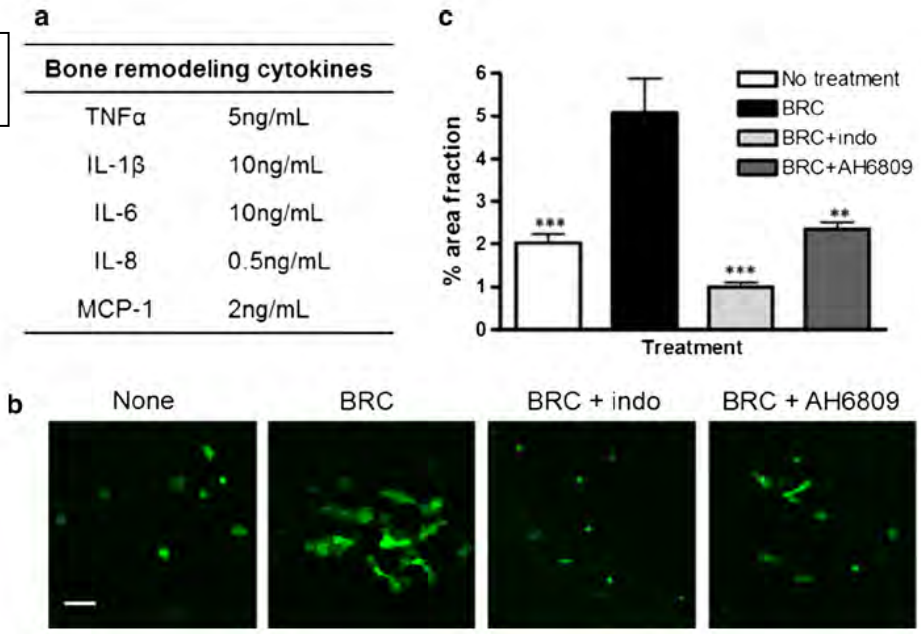

Fig. 4 Bone remodeling cytokines (BRC) induced proliferation of dormant MCF-7 breast cancer cells grown in a 3D osteoblast culture Normal human osteoblasts were grown in the bioreactor for 1 month. The weakly metastatic breast cancer cell line, MCF-7, was added to the growth chamber along with 10 ng/mL bFGF to induce a dormant state. **a** Bone remodeling cytokines TNFα, IL-1β, IL-6, IL-8, and MCP-1 were added to the growth chamber at the concentrations indicated. The COX inhibitor, indomethacin, and the PGE2 receptor antagonist, AH6809, were added to some of the cultures at 50 μM final concentration. **b** Live cell images were captured by confocal microscopy; shown are representative images of day 4 cultures. **c** Area fraction analysis of live cell images on day 4. *Scale bar* 100 microns. n = 6. ***p = 0.001; **p = 0.01 relative to treatment with cytokines

A reported effect of PGE2 on cancer cells in an increase in focal adhesion kinase (FAK). Therefore we examined FAK plaque formation in BRMS1 cells cultured on MC3T3E-1 osteoblasts cultured in the bioreactor with the addition of TNF-α and IL-1β. There was a six fold increase in FAK in the cells in the presence of the cytokines (Figure 16, Figure 5 in appended publication). This value was reduced in the presence of indomethacin.

Figure 16

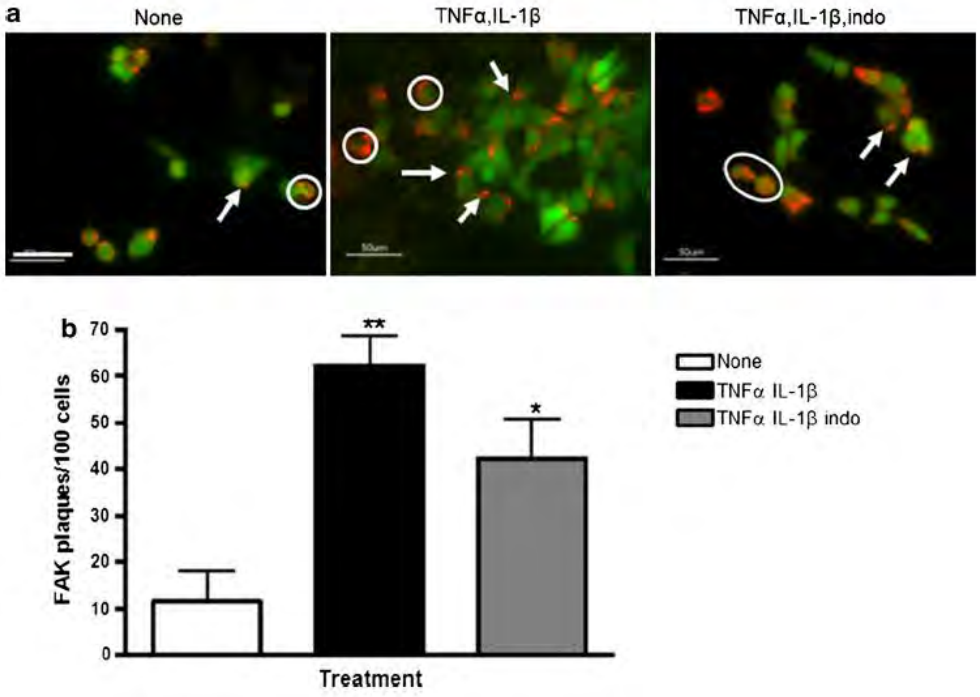

Fig. 5 Focal adhesion plaque formation was increased in co-cultured BRMS1 cells exposed to TNFα and IL-1β. 3D co-cultures of osteoblasts and cancer cells were assembled and treated as described in "Materials and methods" section. After 4 days in culture, bioreactors were disassembled and portions of the membrane stained for phospho-FAK. **a** Cells displaying cytoplasmic distribution of FAK are *circled*; focal adhesion plaques are indicated by *arrows*. *Scale bar* 50 microns. **b** Graph of focal adhesion plaques seen per 100 cells in three fields of view (n = 3). **p = 0.01; *p = 0.05 relative to untreated cultures

Bioreactor culture of normal human osteoblasts (NHOst) and human breast cancer cells

As stated in the 2013 progress report, we were successful in establishing bioreactor cultures of the normal human osteoblasts purchased from Lonza (Walkersville, MD). These cultures produced a rich collagenous matrix and mineralized after one month in culture. However, when MDA-MB-231BRMS1 breast cancer cells were co-cultured with these osteoblasts in the bioreactor, they failed to show the dormancy model seen with the murine osteoblast/ human cancer cell system.

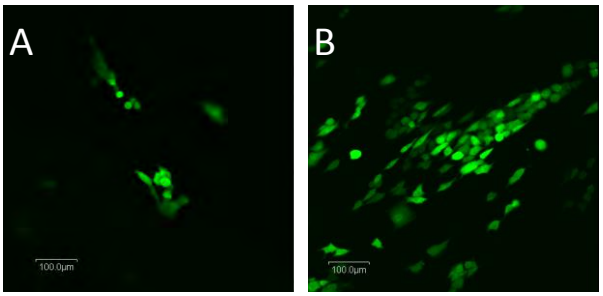

Figure 17. MDA-MB-231BRMS1 breast cancer cells co-cultured for 3 days with MC3T3-E1 murine and NHOst human osteoblasts. A) BRMS1 cancer cells grown on a 2 month old bioreactor culture of MC3T3-E1 osteoblasts. B) BRMS1 cells grown on a 1 month old bioreactor culture of NHOst osteoblasts. Note marked differences in morphology and growth. Scale bar = 100µM.

The MDA-MB-231BRMS cells clearly proliferated and assumed a morphology similar to the aggressive, non-suppressed MDA-MB-231 cells when grown in culture with human osteoblasts . We speculate that the NHOst osteoblasts may be secreting a cytokine or growth factor that is not produced by the MC3T3-E1 osteoblasts that could be triggering proliferation of the cancer cells. Since dormancy could not be established from the outset, this cell pairing proved to be unsuitable as a dormancy model. However, comparison of the two cultures, MC3T3-E1 and NHOst may prove valuable.

The MCF-7 human breast cancer cells proved to be an excellent model to study cancer cell dormancy in a bone-like microenvironment. With the addition of basic FGF, the cells became dormant; the addition of bone remodeling cytokines caused a marked morphological change accompanied by an increase in proliferation. These effects were mitigated by the addition of indomethacin and, to a lesser extent, AH6809. These findings

support the evidence seen in the previous experiment for the important role of bone remodeling cytokines in the awakening of dormant cancer cells.

Bone Cytokine Environment

In order to achieve a more comprehensive understanding of the bone metastatic environment, we designed a series of *in vitro* experiments to examine the intercellular cytokine crosstalk between three breast cancer cell lines, MDA-MB-231, MDA-MB-231BRMS1, MCF-7, and three key cell types of the bone marrow compartment, osteoblasts (NHOst), endothelial cells (BMEC) and stromal cells (KM101). All cell lines were of human origin. Conditioned medium was generated from each of these cell lines. Cultures of each of the bone marrow cell lines were treated with the conditioned media from each of the breast cancer cell lines. Conversely, each cancer cell culture was treated with conditioned medium from each of the three bone marrow cell lines. After 24 hours of treatment with conditioned media or vehicle media, the culture supernatants were collected and assayed for 20 cytokines involved with inflammation and bone remodeling. The MilliPlex (Millipore, Billerica, MA) panel included: epithelial growth factor (EGF), fibroblast growth factor 2 (FGF-2), eotaxin (ETXN), granulocyte colony stimulating factor (G-CSF), fms-like tyrosine kinase 3 (FLT-3L), granulocyte macrophage colony stimulating factor (GM-CSF), fractalkine (FRAK), GROα, platelet-derived growth factor AA and BB (PDGF-AA, PDGF-BB), IL-17A, IL-1β, IL-3, IL-6, IL-8, interferon γ induced protein 10 (IP-10), monocyte chemoattractant protein 1 (MCP-1), RANTES, tumor necrosis factor α (TNFα) and vascular endothelial growth factor (VEGF). The assay plate was run in accordance with the manufacturer's protocol.

The cytokine composition of the conditioned medium for each cell line is summarized in Table 2. All cell lines of the bone marrow compartment secreted IL-6, MCP-1 and VEGF. BMEC and KM101 as well as the cancer cells secrete PDGF-AA. The 231 and BRMS1 cancer cells and the NHOst osteoblasts secrete G-CSF. Interestingly, the less metastatic MCF-7 cells did not. Of particular note is the FGF secreted by the bone marrow stromal cells, KM101. FGF was used in this study's experiments to induce a state of dormancy in MCF-7 cells grown on osteoblasts. When conditioned medium from any of the cancer cell lines was used to treat KM101 stromal cells, FGF levels were reduced by 58%. Results of conditioned media treatments revealed an increase in the inflammatory cytokine IL-6 in all bone marrow cell types when treated with any of the breast cancer cell conditioned media; these media also raised levels of MCP-1 and VEGF in BMEC cultures. While numerous other cytokine levels were affected when the bone marrow cells were treated with cancer cell conditioned media, the cancer cells did not respond to treatment with conditioned media from the cells of the bone microenvironment. The effects of the altered cytokine profile present in the metastatic bone environment will be examined in further detail.

Table 2. Cytokines secreted by human osteoblasts (NHOst), endothelial cells (BMEC), stromal cells (KM101) and breast cancer cell lines, MDA-MB-231 (231), MDA-MB-231BRMS1 (BRMS1) and MCF-7.

Cell line	Secreted cytokines
BMEC	GRO, PDGF-AA, IL-6, MCP-1, VEGF
KM101	FGF, FRAK, PDGF-AA IL-6, MCP-1, VEGF
NHOst	G-CSF, GRO, IL-6, IL-8, MCP-1, RANTES, VEGF
231	G-CSF, PDGF-AA, VEGF
BRMS1	G-CSF, GRO, PDGF-AA IL-8, VEGF
MCF-7	FRAK, PDGF-AA, VEGF

Key Research Accomplishments

- Dormancy models of human metastatic breast cancer in bone were established in a 3D bioreactor system with osteoblasts, both mouse and human.
- Demonstrated that dormancy was broken and the cancer cells grew in the presence of bone remodeling cytokines (TNF-α and IL-1β).
- The downstream target of these cytokines was prostaglandin G2 (PGE2). The break in dormancy could be prevented by indomethacin or a receptor antagonist of PGE2.
- The osteoblast matrix could be manipulated by the amount of estrogen in the culture during osteoblast differentiation.
- Breast cancer cells attached more readily to fixed as opposed to live osteoblast cultures.
- Breast cancer cells grew better in osteoblast cultures grown in the presence of an estradiol receptor antagonist. The cancer cells themselves do not express estrogen receptors.
- Estrogen levels also affected the structure of the collagen and the ratio of collagenous to non-collagenous proteins.
- Cytokine arrays of breast cancer cells, bone marrow stromal cells, bone marrow endothelial cells exposed to conditioned medium from each cell line revealed cytokines that were differentially expressed by each cell type as well as by exposure to another cell type.

Conclusions

While the "five year" cure rate for primary breast cancer is high, many women will die from breast cancer metastases. Very often metastatic breast cancer is found in the skeleton. It appears that the cancer can remain dormant there for many years, even decades. Anecdotal evidence suggests that bone trauma or bone remodeling is associated with breaking of dormancy. In this study we established a dormancy model of human metastatic breast cancer in a three dimensional model of bone. We demonstrated that addition of bone remodeling cytokines TNF-α and IL-1β were sufficient to reawaken the breast cancer cells. These cytokines led to the production of prostaglandin E2, PGE2. Indomethacin, an inhibitor of arachidonic acid pathway, or AH609 a receptor antagonist, prevented the break in dormancy. One of the effects of PGE2 on cancer cells is an increase in focal adhesion kinase. These were increased with TNF-α and IL-1β and reduced with indomethacin.

We also found that the osteoblast matrix in this system could be manipulated by the amount of estrogen present during osteoblast differentiation. Most women who are diagnosed with primary cancer are post-menopausal and thus low in estrogen. In the model system used here, osteoblasts grown with a receptor antagonist of estradiol (i.e. low estrogen), formed a better substrate for attachment of breast cancer cells than a substrate from osteoblast grown in high estrogen. Also matrix that was fixed, i. e. the osteoblasts were present but not alive, were a superior matrix for breast cancer attachment compared to the live matrix.

This *in vitro* work with a 3D model system supports the human data which suggests that aspirin, which also inhibits the arachidonic acid pathway, is worth re-examining for use in breast cancer patients who may be at risk for metastasis. The results of the study with the matrix suggest that the field might re-examine a role for estrogen supplementation under some cases in postmenopausal women.

If we obtain future funding, we plan to continue to characterize the matrix. Physical methods such as atomic force microscopy are available. We also plan to compare the interaction of the metastasis suppressed BRMS cells grown with the mouse matrix (dormancy) and with the human matrix (growth). A comparison will permit

us to determine key elements important in each case. The results of the cytokine array offer some clues as which cancer cells grow or remain dormant. Furthermore, they offer a glimpse into how the cells in the bone marrow compartment can interact.

Publications, Abstracts and Presentations

1. **Lay press:** none
2. **Peer-reviewed Scientific Journals**:
   Sosnoski DM, Norgard RJ, Grove CS, Foster SJ, Mastro AM
   Dormancy and growth of metastatic breast cancer cells in a bone-like microenvironment. Clinical and Experimental Metastasis 32: 335-344, 2015. DOI 10.1007/s10585-015-9710-9; PMID 25749879

   Krishnan, V, Vogler, EA, Sosnoski DM, Mastro AM. In vitro mimics of bone remodeling and the vicious cycle of cancer in bone. Journal of Cellular Physiology 2014 229 :453-62. DOI 10.1002/jcp.24464. PMID 24022654

3 **Invited Articles**: none

4. **Abstracts:**

Kaitlyn Leahy and Andrea M. Mastro. Deadly KISS: Kisspeptin 10 interaction with Osteoblasts and Breast Cancer Metastases. Presented as poster by an undergraduate at American Association for Cancer Research Meetings, April 2014, and at the Eberly COS poster session in the fall of 2014.

Chen, YC, Andrea M Mastro, Donna M Sosnoski, Robert J. Norgard, Cassidy D. Grove and Erwin Vogler. Dormancy and Growth of Metastatic Breast Cancer Cells in a Bone-Like Microenvironment in Vitro. American Association for Cancer Research National Meeting April 2014.

Pursani, Richa, Donna Sosnoski and Andrea M. Mastro. An in vitro study of the chemoattraction between osteoclasts and breast cancer cells. Penn State Undergraduate Research Exhibition , April 2014.

Emily Rutan and Andrea M. Mastro. 2013. The Effects of Bone-Remodeling Cytokines on the Interaction Between Breast Cancer Cells and Osteoblasts on a Bone Matrix In-Vitro. Penn State Undergraduate Research Exhibition , April 2014

Andrea Mastro Penn State Millennium Café “Tracking Metastatic Breast Cancer, Follow the Matrix” June 6, 2014 Penn State

Andrea Mastro Penn State, Biochemistry and Molecular Biology Faculty Talks. “Metastatic Breast Cancer” April 29, 2014.

Shelby J Foster, Donna M Sosnoski, Andrea M. Mastro. Matrix Manipulation Affects Attachment and Growth of Breast Cancer Cells in a Bone-like Microenvironment in Vitro. American Association for Cancer Research, 2015, April 18-22, Philadelphia,PA.

Presentation:

Andrea M. Mastro, Donna M Sosnoski, Y. Chen, R.J. Norgard, C.D. Grove, E. Vogler. Dormancy in a Dish? Growth of metastatic breast cancer cells in a bone-like microenvironment in vitro. Presentation at the 15th International Biennial Congress of the Metastasis Research Society, Heidelberg Germany June 28-July 1, 2014.

Inventions, patents, and licenses: nothing to report

Reportable outcomes: development of a 3D culture system that mimics bone and metastatic cancer interaction. We have contacted several companies regarding possible commercialization.

Other Achievements:

Degrees supported. Several honors students have worked on this project and have since gone on to medical school or to graduate school

Emily Rutan—BS Biochemistry 2014, currently at Tufts Medical School

Ritcha Pursnani—BS Biology 2014, currently at Temple Medical School

Robert Norgard—BS Microbiology 2014, currently University of Pennsylvania Graduate School

Yu-Chi Chen—postdoctoral fellow 2012-2014, currently postdoctoral fellow at Hershey Medical College

Cassidy Grove—BS Biology, currently a senior at Penn State, Nursing

Kaitlyn Leahy—BS Biology, graduating Penn State May 2015, applying to medical school

Shelby Foster—currently an honors student in Biochemistry at Penn State; plans to attend graduate school

Other achievements: Each of the undergraduates received awards ($200-$500 each per year) to help with their research costs; They also were subsidized by the college to attend the AACR meetings

References

Bussard, K.M., D.J. Venzon, and A.M. Mastro. 2010. Osteoblasts are a major source of inflammatory cytokines in the tumor microenvironment of bone metastatic breast cancer. *Journal of cellular biochemistry*. 111:1138-1148.

Carlsten, H. 2005. Immune responses and bone loss: the estrogen connection. *Immunological reviews*. 208:194-206.

Gehler, S., S.M. Ponik, K.M. Riching, and P.J. Keely. 2013. Bi-directional signaling: extracellular matrix and integrin regulation of breast tumor progression. *Critical reviews in eukaryotic gene expression*. 23:139-157.

Krishnan, V., E.A. Vogler, D.M. Sosnoski, and A.M. Mastro. 2014. In vitro mimics of bone remodeling and the vicious cycle of cancer in bone. *Journal of cellular physiology*. 229:453-462.

Mastro, A.M., and E.A. Vogler. 2009. A Three-Dimensional Osteogenic Tissue Model for the Study of Metastatic Tumor Cell Interactions with Bone. *Cancer research*. 69:4097.

Mitchell, K., K.B. Svenson, W.M. Longmate, K. Gkirtzimanaki, R. Sadej, X. Wang, J. Zhao, A.G. Eliopoulos, F. Berditchevski, and C.M. Dipersio. 2010. Suppression of integrin alpha3beta1 in breast cancer cells reduces cyclooxygenase-2 gene expression and inhibits tumorigenesis, invasion, and cross-talk to endothelial cells. *Cancer research*. 70:6359-6367.

Zong, Y., Y. Xu, X. Liang, D.R. Keene, A. Hook, S. Gurusiddappa, M. Hook, and S.V. Narayana. 2005. A 'Collagen Hug' model for Staphylococcus aureus CNA binding to collagen. *The EMBO journal*. 24:4224-4236.

Clin Exp Metastasis (2015) 32:335–344
DOI 10.1007/s10585-015-9710-9

RESEARCH PAPER

Dormancy and growth of metastatic breast cancer cells in a bone-like microenvironment

Donna M. Sosnoski[1] · Robert J. Norgard[1] · Cassidy D. Grove[1] · Shelby J. Foster[1] · Andrea M. Mastro[1]

Received: 23 December 2014 / Accepted: 28 February 2015 / Published online: 8 March 2015

Abstract Breast cancer can reoccur, often as bone metastasis, many years if not decades after the primary tumor has been treated. The factors that stimulate dormant metastases to grow are not known, but bone metastases are often associated with skeletal trauma. We used a dormancy model of MDA-MB-231BRMS1, a metastasis-suppressed human breast cancer cell line, co-cultured with MC3T3-E1 osteoblasts in a long term, three dimensional culture system to test the hypothesis that bone remodeling cytokines could stimulate dormant cells to grow. The cancer cells attached to the matrix produced by MC3T3-E1 osteoblasts but grew slowly or not at all until the addition of bone remodeling cytokines, TNFα and IL-β. Stimulation of cell proliferation by these cytokines was suppressed with indomethacin, an inhibitor of cyclooxygenase and of prostaglandin production, or a prostaglandin E2 (PGE2) receptor antagonist. Addition of PGE2 directly to the cultures also stimulated cell proliferation. MCF-7, non-metastatic breast cancer cells, remained dormant when co-cultured with normal human osteoblast and fibroblast growth factor. Similar to the MDA-MB-231BRMS1 cells, MCF-7 proliferation increased in response to TNFα and IL-β. These findings suggest that changes in the bone microenvironment due to inflammatory cytokines associated with bone repair or excess turnover may trigger the occurrence of latent bone metastasis.

✉ Andrea M. Mastro
a36@psu.edu

[1] Department of Biochemistry and Molecular Biology, The Pennsylvania State University, 428 S. Frear Laboratory, University Park, PA 16802, USA

Keywords Breast cancer · Dormancy · Three-dimensional bioreactor · Bone metastases · Prostaglandins

Introduction

The 5 year cure rate for localized breast cancer is high, e.g. 99 % [1]. However, this figure belies the fact that breast cancer can reoccur as metastatic disease many years and even decades after the original treatment [2, 3]. Once relapse occurs, and the cancer colonizes in distant organs, the relative survival rate drops to 24 % [1]. One of the preferred metastatic sites for breast cancer is the skeleton. It is estimated that 65–75 % of individuals with advanced disease harbor bone metastases [4], and that over 70 % of patients dying from breast cancer have evidence of bone metastases at post-mortem examination [5]. In fact, it has been suggested that many patients have undetected disseminated tumor cells (DTC) or micro-metastases at the time of diagnosis of the primary tumor [6]. There is evidence that the process of primary tumor resection may trigger metastasis [7]. Indeed, the bone may provide a transient niche from which metastatic cells may later seed other secondary organs [8].

Not all DTC that lodge in secondary organs will grow. The efficiency of metastasis is estimated to be low [9]. Dissemination alone is not sufficient to cause formation of "…overt, vascularized, clinically detectable metastases" [10, 11]. Cancer cells can remain dormant in secondary organs for long periods, often years or even decades depending on the tumor [2, 12]. There are reports of the transfer of DTC to patients through organs transplanted from individuals either not known to have cancer or thought to be cured for many years. These occult DTC then grew in the immunosuppressed recipient (see [2]). It is

estimated that 30 % of breast cancer patients diagnosed at the MO tumor-node-metastasis tumor stage already contain DTC in their bone marrow [10]. Dormant cells apparently survive chemotherapy, radiation and adjuvant therapy, and may reawaken at a later time and proliferate as bone metastases. The prediction of metastatic recurrence is poor at best. Current estimates are based on the phenotype of the tumor and use of circulating tumor cells (CTC) as prognostic indicators [13, 14]. The numbers of these CTC as well as their gene signatures are being used to develop predictive algorithms. However, the results are far from definitive [15]. Identification of the factors that either maintain the dormant state or cause dormant cells to proliferate is crucial to the development of clinical strategies to prevent recurrence of malignancy.

There is evidence that disruption of the dormant tumor cell niche may trigger recurrence of dormant cells many years after primary treatment. Local trauma, wounding, or injury may spur tumor cells to grow. Chronic inflammation and/or immunosuppression also are important factors to be considered in cancer recurrence (reviewed by [6]). Das Roy et al. found an increase in lung and bone marrow metastasis using an arthritic mouse model [16]. Recently, Yano [17] reported the case of a woman who experienced breast cancer relapse 24 years after mastectomy and radiation treatment, when administered drugs for rheumatoid arthritis. In another case, [18] a tracheostomy wound was the site of breast cancer outgrowth for a woman 10 years after mastectomy. In fact, it was recognized over a century ago that the surgical process employed to remove the primary tumor might itself promote metastasis (reviewed by [19]). There is also evidence that recombinant PTH (aa 1-34) which enhances bone turnover, also causes increased bone metastasis in rodents and possibly in humans [20, 21].

Given this anecdotal evidence, we speculated that cytokines involved in bone remodeling and repair post trauma [22] play a role in the growth of dormant breast cancer cells in the bone. For this study, we used a specialized three-dimensional (3D) model of an in vitro bone mimic that permits the growth of a multiple layer of mineralized osteoblast tissue from pre-osteoblasts [23]. We had observed that a human metastatic breast cancer cell line, MDA-MB-231 [24], grows in this chamber in a manner that mimics metastatic breast cancer growth in bone [25]. However, a metastasis suppressed variant, MDA-MB-231BRMS1 [26], does not readily grow in this same bone-like environment [27]. The BRMS1 variant shows this same property in mice; i.e. in an experimental model of metastasis, the BRMS1 cells are detected in the bone marrow but seldom grow there [28, 29]. The weakly metastatic human breast cancer cell line, MCF-7, has also been used as a model for breast cancer cell dormancy [30]. In this model, the addition of fibroblast growth factor (FGF) to MCF-7 cells grown on matrigel causes the cells to enter a state of dormancy.

In the bone microenvironment, cytokines play a vital role in bone turnover, remodeling, and repair. Transforming growth factor α (TNFα), interleukin 1β (IL-1β) and interleukin 6 (IL-6) are reported to be key signaling molecules in the multistep process of bone remodeling [20]. Furthermore, TNFα and IL-1β are known to stimulate production of prostaglandin E2 (PGE2), an important inflammatory molecule, in numerous cell types including osteoblasts [31, 32]. PGE2, in turn, is known to upregulate the production and phosphorylation of focal adhesion kinase (FAK) [33] which plays a key role in cell adhesion, motility and survival.

In our current study, addition of a cocktail of bone remodeling cytokines to the 3D dormancy model cultures resulted in a marked increase in proliferation of the breast cancer cells in both culture systems. The proliferative effect was also seen with the addition of exogenous PGE2. However, a dormant state was maintained in the presence of the cytokines with the addition of indomethacin, a COX inhibitor or AH6809, a PGE2 receptor antagonist. Increased formation of focal adhesion kinase plaques by the cancer cells treated with bone remodeling cytokines was also observed.

Materials and methods

Cell culture

The human metastatic breast cancer cell line, MDA-MB-231 [24] and its metastasis-suppressed variant, MDA-MB-231BRMS1 [26] were gifts of Dr. Danny Welch, University of Kansas Cancer Center. MDA-MB-231 cells were cultured in DMEM (Corning Cellgro, Manassas, VA), 5 % fetal bovine serum (PAA Laboratories, Etobicoke, Ontario), 1 % non-essential amino acids (Corning Cellgro) and penicillin/streptomycin (Corning Cellgro) at 100 IU/mL and 100 mg/mL concentration, respectively. MDA-MB-231BRMS1 cells were grown in DMEM/F12, 5 % FBS, 1 % NEAA and penicillin/streptomycin. The cell line, MCF-7 [30], was a gift from Dr. Robert Wieder, Rutgers University, and was propagated in DMEM, 10 % FBS, penicillin/streptomycin. All cancer cell lines were engineered to express green fluorescent protein (GFP). The murine osteoblast precursor cell line, MC3T3-E1 [34], was provided by Dr. Norman Karin, University of Texas, and was propagated in α MEM (Corning Cellgro), 10 % FBS and penicillin/streptomycin. In order to differentiate the osteoblasts, 10 mM β-glycerophosphate and 50 μg/mL ascorbic acid were added to the medium. Normal human osteoblasts, NHOst, and the proprietary growth and differentiation media were purchased

from Lonza (Walkersville, MD) and grown according to their protocol.

Osteoblast bioreactor cultures were established as previously described [23]. In brief, 10,000 cells/cm^2 of either MC3T3-E1 or NHOst were seeded in the growth chamber of the bioreactor in the appropriate differentiation medium containing either 10 % (MC3T3-E1) or 15 % (NHOst) fetal bovine serum. The upper medium reservoir was filled with differentiation medium without serum and was replaced every 2–3 weeks. MC3T3-E1 cultures were maintained for 2 months; NHOst cultures for 1 month.

Cytokine and cancer cell addition

All cytokines and neutralizing antibodies were purchased from R&D Systems (Minneapolis, MN). PGE2 was obtained from Cayman Chemical (Ann Arbor, MI). The bone remodeling cytokine cocktail for the MC3T3-E1/BRMS1 dormancy model initially consisted of TNFα (5 ng/mL), IL-1β (10 ng/mL), IL-6 (10 ng/mL) and PGE2 (100 nM), but was later reduced to TNFα and IL-1β. The remodeling cytokines for the NHOst/MCF-7 model was composed of TNFα (5 ng/mL), IL-1β (10 ng/mL), IL-6 (10 ng/mL), IL-8 (0.5 ng/mL) and MCP-1(2 ng/mL). In addition, 10 ng/mL basic fibroblast growth factor (bFGF) was added to the NHOst/MCF7 cultures to establish dormancy. For neutralizing antibody experiments, anti-human TNFα, IL-1β, and IL-6 were added at concentrations of 5, 20, and 0.6 μg/mL, respectively. Cytokines and neutralizing antibodies were added to the growth chamber only. The cyclooxygenase inhibitor, indomethacin, purchased from Sigma-Aldrich (St. Louis, MO), was added to both chambers of the bioreactors at a concentration of 50 μM. The PGE2 receptor antagonist, AH6809, was obtained from Cayman Chemical and used at a concentration of 50 μM in both reactor chambers.

Cytokines and inhibitors were added to the bioreactor osteoblast cultures. Approximately 15 min after their addition, the MDA-MB-231 or MDA-MB-231BRMS1 cells at a concentration of 4000 cells/cm^2 were added to the mature murine osteoblast cultures; MCF-7 cells were added to the NHOst cultures at a concentration of 2000 cells/cm^2. The medium in the upper reservoir was replaced with fresh differentiation medium at the same time.

Live cell imaging

Bioreactor cultures were imaged daily for 3–4 days of the co-culture period using the Olympus FV300 confocal microscope at a 200× magnification. Three to six representative images were captured for each bioreactor culture at each time point. Images were analyzed by ImageJ [35] using area fraction quantitation methodology. Statistical analyses were performed with GraphPad Prism 4.0 using two-way ANOVA with Bonferroni correction.

Prostaglandin E2 assay

The level of PGE2 in the bioreactor culture supernatants was measured by a competitive enzyme immunoassay method (GE Healthcare, Piscataway, NJ).

Immunocytochemistry

After 3–4 days of co-culture, the bioreactors were disassembled. The growth chamber membrane with attached cells and matrix was carefully excised from the device and rinsed once with PBS. The membrane was then fixed in 4 % paraformaldehyde (Electron Microscopy Sciences, Hatfield, PA) and stored at 4 °C. Culture membranes were divided into small portions for immunostaining.

The primary rabbit antibodies to Ki67 (ab927442) and focal adhesion kinase (phospho Y397; ab4803) were purchased from Abcam (Cambridge, MA). A goat anti-rabbit IgG antibody conjugated to Alexa 568 (Life Technologies, Grand Island, NY) was used for detection. Briefly, membrane fragments were rinsed in PBS. Cells were permeabilized in 0.05 % triton X-100 in PBS for 15 min then washed in PBS and blocked in PBS containing 10 % normal goat serum (NGS) for 1 h. Antibodies for Ki67 and FAK were diluted in PBS 1 % NGS at 1:300 and 1:100, respectively, and applied to the membranes for 2 h. After washing the membranes three times with PBS, the secondary goat anti-rabbit IgG Alexa 568 was diluted 1:200 in PBS 1 % NGS and applied for 1 h. Membranes were washed 3 times in PBS and mounted on glass slides with Fluoromount G (Southern Biotech, Birmingham, AL). Slides were imaged using a Keyence BZ-X700 fluorescence microscope with 60× and 100× lenses.

Results

Bone remodeling cytokines stimulated the proliferation of MDA-MB-231BRMS1 cells

A cocktail of cytokines reported to be present during bone remodeling [22, 36, 37], TNFα (5 ng/mL), IL-1β (10 ng/mL), IL-6 (10 ng/mL) and PGE2 (100nM), was added to 2 month old bioreactor cultures of MC3T3-E1 (Fig. 1a). Approximately 15 min later MDA-MB-231^{-GFP} or MDA-MB231BRMS1^{-GFP} cells were added to the cell growth chambers. The co-cultures were examined daily by confocal microscopy for 4 days. As seen previously, the cells attached to the matrix. The cytokine treatment had no obvious effect on the growth or appearance of the 231 cells. However, the

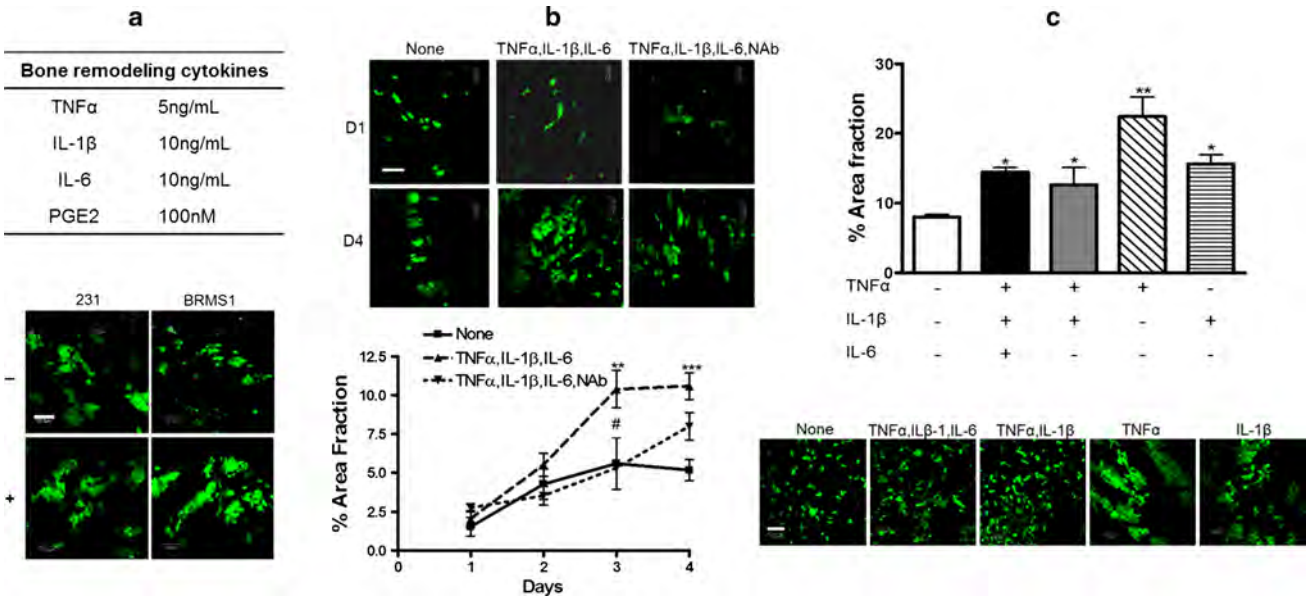

Fig. 1 Bone remodeling cytokines increased the growth and affected the morphology of MDA-MB-231BRMS1 breast cancer cells grown in a 3D osteoblast culture The bone remodeling cytokine cocktail, consisting of TNFα, IL-1β, IL-6, and PGE2, was added to a 2 month old, 3D culture of MC3T3-E1 murine osteoblasts 15 min prior to the addition of 10^5 MDA-MB231^{GFP} or MDA-MB-231BRMS1^{GFP} human breast cancer cells. Live images of the co-cultures were collected daily using confocal microscopy. Image quantitation was performed using ImageJ; statistical analysis was performed using GraphPad Prism. **a** Representative images of day 4 co-cultures of 231 or BRMS1 cells with and without the bone remodeling cytokine cocktail (n = 3). **b** Images and area fraction graph of BRMS1 osteoblast co-cultures incubated with TNFα, IL-1β, and IL-6 with and without addition of neutralizing antibodies (NAb) to the three cytokines. Shown are representative images from days 2 and 4 of co-culture (n = 3). **c** Representative day 3 images and area fraction analysis of BRMS1 co-cultures with TNFα and/or IL-1β additions (n = 3). *Scale bar* 100 microns. ***p = 0.001; **p = 0.01; *p = 0.05 when comparing cultures with and without cytokines. #p = 0.01 when comparing cultures with cytokines to cultures with cytokines and NAb. n = 3

BRMS1 cells grew into large multicellular colonies in comparison to little or no growth in the absence of added cytokines (Fig. 1). This growth pattern was similar to that observed for untreated metastatic 231 cells.

Because TNFα, IL-1β, and IL-6 can activate the arachidonic acid pathway leading to production of prostaglandins [38–40], we omitted PGE2 from the cocktail and repeated the experiment (Fig. 1b). Over four days of culture without added cytokines, there was a small increase in the area fraction occupied by the BRMS1 cells indicative of slow growth over time. Addition of TNFα, IL-1β, and IL-6 was sufficient to enhance the growth of the BRMS1 cells without the inclusion of PGE2. By day four of culture, the cells had increased more than twofold over those with no cytokines added. The addition of neutralizing antibodies (Nab) to TNFα, IL-1β and IL-6 at the beginning of the co-culture period prevented the increase in proliferation elicited by the cytokines, at least for the first 3 days of culture (Fig. 1b).

In order to further narrow down the list of effector cytokines, we tested TNFα and IL-1β in tandem and individually. We had previously observed that IL-6 had no effect on BRMS1 growth (data not shown). TNFα and IL-1β alone or together caused an increase in BRMS1 colony formation (Fig. 1c). The increase in growth compared to cultures without cytokines ranged from two to four fold.

Prostaglandin E2 was the effector molecule

Because both TNFα and IL-1β can initiate the arachidonic acid pathway, we asked if indomethacin, an inhibitor of COX1 and COX2, could block the growth response of BRMS1 cells to these cytokines. In this set of experiments, TNFα and IL-1β increased growth of BRMS1 cells in the cultures by over sevenfold at day four when compared to cells grown without added cytokines (Fig. 2a). The addition of 50 μM indomethacin prevented the cytokine-induced increase. Indomethacin alone did not affect cell growth (Fig. 2a). Interestingly, indomethacin also appeared to suppress colony formation; the cells remained as single cells or small clusters. Because PGE2 is the major downstream molecule produced by COX2 AH6809, an antagonist to the PGE2 receptor, was employed to investigate the role of PGE2 in the growth-promoting effects of TNFα and IL-1β on the BRMS1 cells. AH6089 (50 μM) was added to 3D cultures simultaneously with the cytokines (Fig. 2b). As seen previously, cultures containing TNFα and IL-1β contained about twice as many cells as untreated

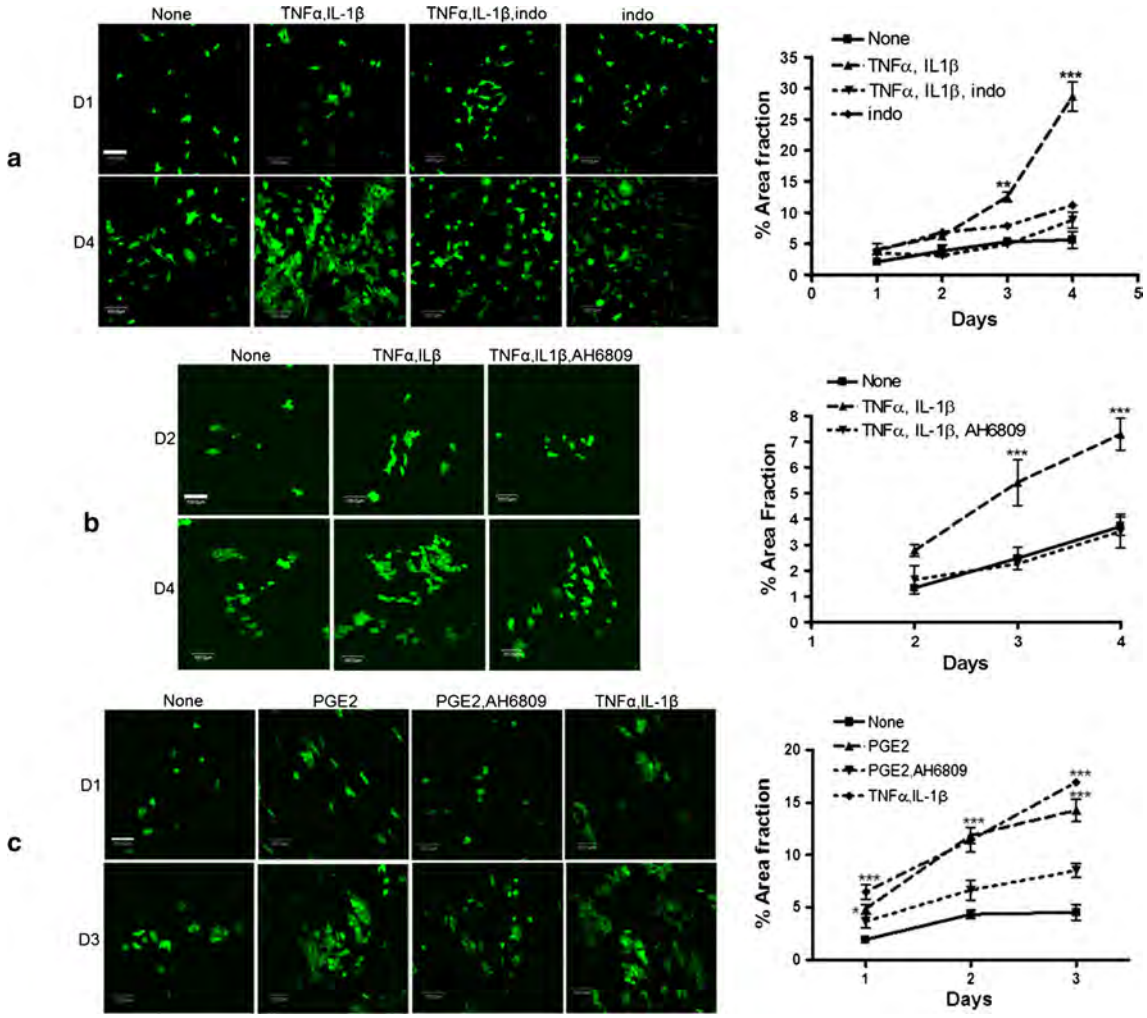

Fig. 2 Indomethacin or the PGE2 receptor inhibitor AH6809 blocked the proliferative effects of TNFα and IL-1β or PGE2 on BRMS1 breast cancer cell in a 3D osteoblast culture **a** TNFα, IL-1β, and BRMS1 cells were added to the 3D cultures and imaged as previously described. The cyclooxygenase inhibitor, indomethacin, was added at a concentration of 50 μM to some of the cultures prior to the addition of the cancer cells. Shown are day 2 and 4 images along with % area fraction plotted over time. **b** The PGE2 receptor antagonist (50 μM), AH6809, was added to co-cultures containing TNFα and IL-1β. Shown are images of day 2 and 4 with area fraction analysis graph. **c** Images and area fraction analysis of co-cultures containing TNFα, IL-1β or 300 nM PGE2; AH6809 was added to some cultures. *Scale bar* 100 microns. ***p = 0.001; **p = 0.01 relative to untreated cultures. n = 3 for (**a**) and (**b**); n = 6 for (**c**)

cultures. This increase in growth was mitigated by AH6809 (Fig. 2b). As with indomethacin, AH6089 alone did not affect the growth of the BRMS1 cells (data not shown).

These data suggested that TNFα and IL-1β stimulated BRMS1 growth via PGE2 production. Collected bioreactor culture supernatants were assayed for the presence of PGE2 (Table 1). We found that untreated bioreactors of MC3T3-E1 with or without BRMS1 cells contained approximately 500 pg/mL of PGE2. Addition of TNFα and IL-1β increased the concentration by 60–70 fold to approximately 35 ng/mL. This increase was prevented by addition of NAb to TNFα and IL-1β, and by indomethacin, but not by AH6809.

In order to determine if PGE2 alone was sufficient to cause increased BRMS1 growth, 300nM PGE2 (approximately 35 ng/mL) was added directly to the BRMS1/3D bone mimetic culture. PGE2 alone brought about a significant increase in BRMS1 cell proliferation (Fig. 2c). The threefold increase was similar to that seen with TNFα

Table 1 Production of PGE2 in bioreactor cultures of MDA-MB-231BRMS1 cells with MC3T3-E1

Treatment	PGE2 (pg/mL) ± SD
None	518 ± 2
TNFα, IL-1β	35,108 ± 115
TNFα, IL-1β, NAb	368 ± 171
TNFα, IL-1β, indo	379 ± 71
TNFα, IL-1β, AH6809	32,450 ± 2963
Untreated MC3T3-E1	522 ± 10

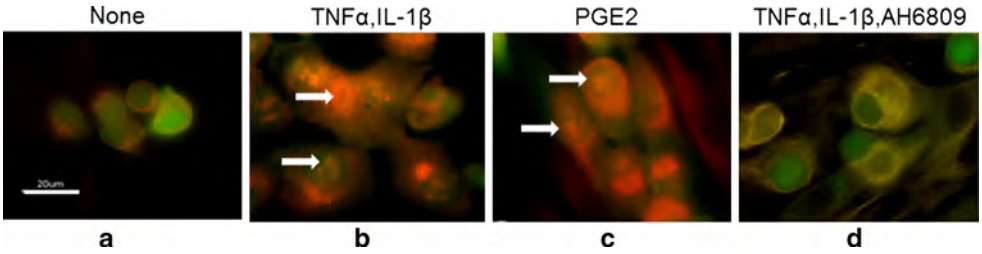

Fig. 3 Nuclear localization of the proliferation marker, Ki67, was increased in co-cultured BRMS1 cells exposed to TNFα and IL-1β or PGE2 Co-cultures were assembled and treated as described in the "methods" section. After 4 days, cultures were disassembled; segments of the culture membrane were fixed and stained by fluorescent immunocytochemistry for the presence of Ki67. Percentage of cells positive for Ki67 nuclear staining was determined from 50 cells per treatment group. Shown are images from **a** untreated culture (2 %) and cultures treated with **b** TNFα and IL-1β (28 %), **c** PGE2 (24 %) or **d** TNFα, IL-1β and PGE2 receptor inhibitor AH6809 (0 %). Positive nuclear staining is indicated by *arrows*. *Scale bar* 20 microns

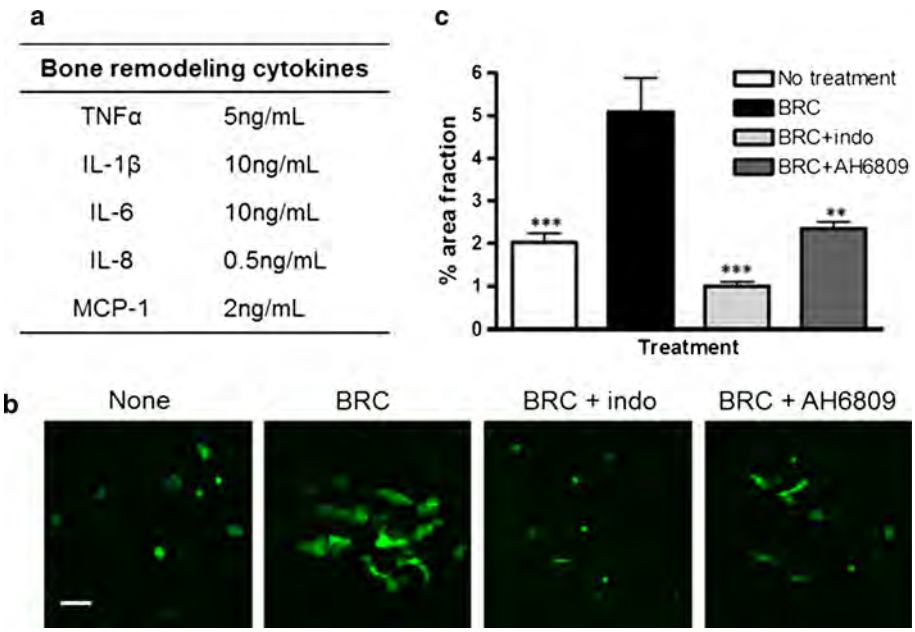

Fig. 4 Bone remodeling cytokines (BRC) induced proliferation of dormant MCF-7 breast cancer cells grown in a 3D osteoblast culture Normal human osteoblasts were grown in the bioreactor for 1 month. The weakly metastatic breast cancer cell line, MCF-7, was added to the growth chamber along with 10 ng/mL bFGF to induce a dormant state. **a** Bone remodeling cytokines TNFα, IL-1β, IL-6, IL-8, and MCP-1 were added to the growth chamber at the concentrations indicated. The COX inhibitor, indomethacin, and the PGE2 receptor antagonist, AH6809, were added to some of the cultures at 50 μM final concentration. **b** Live cell images were captured by confocal microscopy; shown are representative images of day 4 cultures. **c** Area fraction analysis of live cell images on day 4. *Scale bar* 100 microns. n = 6. ***p = 0.001; **p = 0.01 relative to treatment with cytokines

and IL-1β (3.7 fold). The cells also formed colonies similar to those seen in the presence of TNF-α and IL-1β. This increase in cell proliferation, colony formation and shape was prevented when the PGE2 receptor antagonist, AH6809, was present in the culture mix.

In order to verify the proliferative state of the BRMS1 cells under the various conditions, immunocytochemical detection of Ki67 was carried out on the co-cultured cells (Fig. 3). In untreated cultures, there was a minimal (2 %) number of BRMS1 cells with nuclear localization of Ki67 (Fig. 3a). Conversely, in cultures containing TNFα and IL-1β (Fig. 3b) or PGE2 (Fig. 3c) Ki67 was localized in the nucleus of 28 % and 24 % of the cells, respectively. AH6809 prevented Ki67 nuclear localization (0 %) in the presence of TNFα and IL-1β (Fig. 3d).

Bone remodeling cytokines stimulated proliferation of dormant cells in the MCF-7 model

MCF-7 is a human, ER+, breast cancer cell line, used to model dormancy in the presence of fibroblast growth factor, FGF [41]. In our 3D bone model, these cells entered a dormant state when co-cultured with either normal human osteoblasts (NHOst) or MC3T3-E1 with 10 ng/mL FGF (see Fig. 4b and

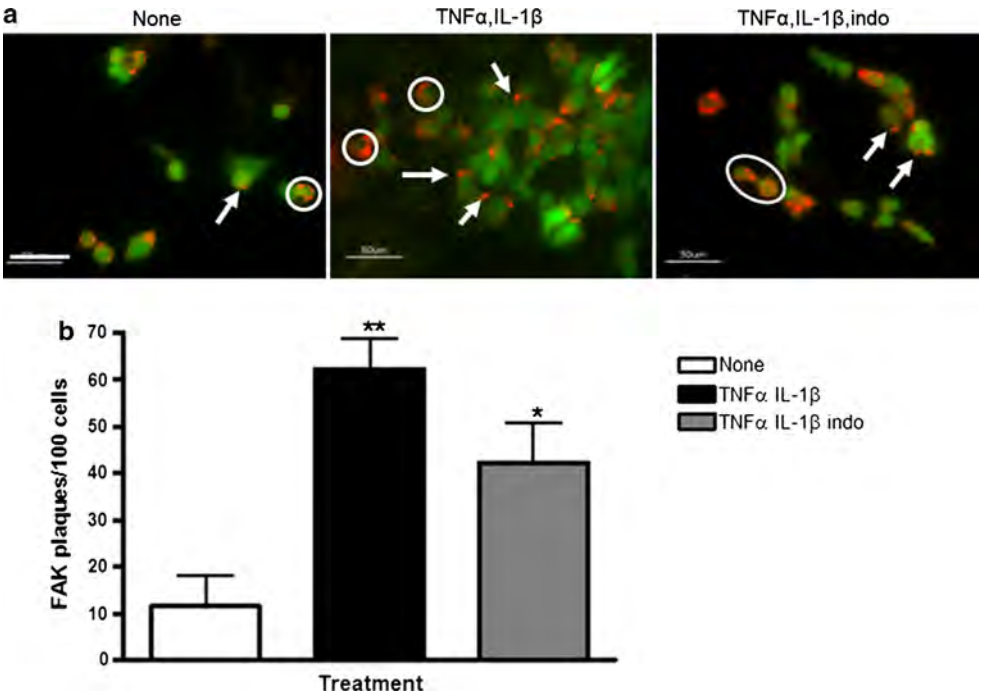

Fig. 5 Focal adhesion plaque formation was increased in co-cultured BRMS1 cells exposed to TNFα and IL-1β. 3D co-cultures of osteoblasts and cancer cells were assembled and treated as described in "Materials and methods" section. After 4 days in culture, bioreactors were disassembled and portions of the membrane stained for phospho-FAK. **a** Cells displaying cytoplasmic distribution of FAK are *circled*; focal adhesion plaques are indicated by *arrows*. *Scale bar* 50 microns. **b** Graph of focal adhesion plaques seen per 100 cells in three fields of view (n = 3). **p = 0.01; *p = 0.05 relative to untreated cultures

data not shown). A panel of human bone remodeling cytokines (Fig. 4a) was tested in the MCF-7/NHOst system to determine if proliferation was catalyzed as in the MC3T3-E1/BRMS system. As predicted, the MCF-7 cells broke dormancy and proliferated in the presence of the cytokines (Fig. 4b). While untreated cells remained in small clumps, cells treated with cytokines expanded into larger colonies. As seen with the BRMS1 cells, both indomethacin and AH6809 prevented this change in proliferation and colony formation (Fig. 4b, c).

Focal adhesion kinase plaque formation was upregulated by TNFα/IL-β in BRMS1 dormancy model

One of the reported effects of PGE2 on cancer cells is an increase in focal adhesion kinase (FAK) plaque formation [33]. Therefore, we examined FAK plaque formation in BRMS1 cells cultured on MC3T3-E1 osteoblasts in the 3D chamber with addition of TNFα and IL-1β (Fig. 5). The increase in plaque formation in the presence of cytokines (Fig. 5a, center) was clearly seen when compared with cultures with no additions (Fig. 5a, right) or with cytokines plus indomethacin (Fig. 5a, left). Furthermore, the cytokine-treated cells displayed a distinctly different morphology than the untreated or indomethacin treated cells. Quantification of the FAK plaques revealed an approximately sixfold increase in plaques in the cells treated with TNFα and IL-1β over those without cytokines. Indomethacin reduced plaque formation, but failed to restore it to the untreated level (Fig. 5b).

Discussion

In summary, we have used a 3D model of a bone mimic to investigate possible mechanisms for breast cancer cell dormancy and recurrence in the bone. Two cancer cell dormancy models, MDA-MB-231BRMS1 and MCF-7, were utilized. In previous studies in mice, BRMS1 formed primary tumors and trafficked to the bone when introduced by intracardiac injection where they appeared to remain dormant [29, 42]. Additionally, these cells grew poorly on an 3D osteoblastic matrix [27]. However, addition of a set of cytokines associated with bone repair and remodeling, specifically TNFα and IL-1β, induced the BRMS1 cells to proliferate. In the presence of TNFα and IL-β, the co-cultures were discovered to produce large amounts of PGE2. Inhibition of PGE2 production with indomethacin or blocking its receptor reversed the cytokine effect on BRMS1 proliferation. Addition of exogenous PGE2 also caused the cells to break dormancy and proliferate. Similar findings were seen with a non metastatic cell line, MCF-7 grown on human osteoblasts in the 3D culture system. These data suggest that PGE2 is a key effector in the breast cancer cell "dormant-to-proliferative" transition in the bone microenvironment.

Prostaglandin E2, the major product of activation of COX-2, plays an important role in normal bone physiology as well as in cancer and bone metastasis (review [43]). In the normal bone, PGE2 is the major prostaglandin and is a strong stimulator of both bone resorption and bone production. It is also elevated under conditions of inflammation

associated with diseases such as rheumatoid arthritis. Moreover, high levels of COX-2 and PGE2 are indicators of poor prognosis for breast cancer patients [44]. COX-2 is reported to be expressed in 40 % of human invasive breast cancers [45].

It has been known for many years that malignant breast cancer cells produce high levels of prostaglandins [46]. Results of studies with mice have provided strong evidence that COX-2 expression is important in bone metastasis. In one study, it was found that breast cancer cells recovered from metastases in the bone produced more prostaglandins than the cell line initially injected into the mice; COX-2 overexpressing breast cancer cells enhanced bone metastases; and finally, an inhibitor of COX-2 reduced the formation of bone metastases [45].

Our data support the premise that BRMS1 cells remain dormant, in part, because they do not produce COX-2 and therefore, PGE2. In fact, Cicek et al. reported that the BRMS1 protein inhibits activation of NF-κB and expression of COX-2 [47]. In a comparison study of MDA-MB-231 and MDA-MB-231BRMS1 cells, they found that BRMS1 cells showed reduced expression of both constitutively produced and TNFα-induced NF-κB. Since COX-2 expression is an indicator of NF-kB activity and PGE2 production dependent on COX-2, we can infer that PGE2 likely plays a major role in the BRMS1 dormancy model. The source of the elevated PGE2 levels seen in the bioreactor is likely the osteoblasts rather than the cancer cells. MC3T3-E1 cultured alone or together with BRMS1 in the bioreactor without additional cytokines produce approximately the same levels of PGE2 (Table 1). It has been known for some time that MC3T3-E1 produce PGE2 when stimulated by TNFα or IL-1β [31, 32]. Although, TNFα and IL-1β bind to different receptors, they are known mediators of bone resorption [48]. Interestingly, it also has been reported that MCF-7 cells do not express COX-2 [49] which may, in part, explain their non metastatic potential.

Clinical dormancy of breast cancer is well known and documented. However, this phenomenon is notoriously difficult to study. From an experimental approach, dormancy is often considered as cellular, angiogenic, or immune related [50]. Cellular refers to mechanisms that keep cells in a quiescent state. Angiogenic dormancy suggests the lack of vascularization limits tumor mass. Immune mediated dormancy implies that host immunosurveillance normally keeps the tumor cells in check. In reality, all of these mechanisms and others are likely involved. In this study, we focused on cellular dormancy as dictated by the local microenvironment.

Many environmental factors can influence metastasis including those produced during resection of the primary tumor [19]. Stress of various kinds can change the environmental milieu of hormones and cytokines. Under normal conditions, hematopoietic stem cells, HSC, reside in the bone in a dormant state. However, it is known that normal cell turnover as well as injury and stress can activate these cells [51]. There is evidence that metastasized cancer cells occupy the same niche as HSC in the bone [52]. Perhaps the metastases respond to the same stress signals.

Focal adhesion kinase is a PTK2 protein tyrosine kinase, encoded by the *PTK2* gene. This kinase concentrates in focal adhesions that form as cells attach to the extracellular matrix. When FAK is reduced, breast cancer cells are less metastatic due to decreased mobility [53]. FAK foci are affected by integrin activation, growth factor stimulation, and action of mitogenic neuropeptides. PGE2 has been reported to increase focal adhesion kinase in breast cancer [33] a phenomenon observed in this study when the BRMS1 were treated with the bone remodeling cytokines TNFα and IL-1β.

In the 3D model system reported in this study consisting of MDA-MB-231BRMS1 cells co-cultured with a well differentiated osteoblast matrix, BRMS1 behaved as dormant cells; i.e. they did not proliferate. However, addition of cytokines, TNFα and IL-1β, that stimulate production of PGE2, led to a break in dormancy resulting in cell proliferation as evidenced by nuclear localization of Ki67. Addition of PGE2 directly to the cultures had the same effect. Moreover, inhibition of COX or the PGE2 receptor prevented cell proliferation. A downstream effect of increased PGE2 activity is a corresponding increase in focal adhesion kinase plaque formation resulting in increased cell spreading and matrix adhesion. Although PGE2 is required for normal bone homeostasis, elevated levels in the bone microenvironment may trigger dormant breast cancer cells to proliferate. The results of this study provide a plausible explanation for the emergence of latent metastases following skeletal trauma. It is under conditions such as bone repair in which there is an osteoblast inflammatory response, that large amounts of PGE2 are produced locally. These findings provide evidence for dormant cells growth following exposure to specific inflammatory cytokines that elevate local concentrations of PGE2.

In a 2009 review, Naumov et al. [6]. discuss clinical dormancy and possible mechanisms. They point out that many individuals carry microscopic tumors that remain dormant for life. A summary of autopsy studies of individuals who died of trauma indicated that as many as 39 % of the women over 39 years of age harbored microscopic breast cancer. Similar incidents were seen with prostate and thyroid cancers. The authors present case studies where trauma was linked to the rapid appearance of lymphomas which had apparently been occult for years. As we pointed out in the introduction, there are other case studies of individuals in which metastasis occurs many years after

removal of the primary tumor and following trauma or disease of the immune system (e.g. [17]). In summary, there is compelling clinical evidence that cancer cell dormancy exists and that bone trauma may trigger the proliferation of the disseminated cells. However, this clinical phenomenon is difficult to study and valid mouse models are not presently available [54]. The 3D culture system described herein offers an in vitro approach to begin to dissect some of the mechanisms related to dormancy with the possibility of creating an animal model in the future.

Acknowledgments This work was supported by a pilot grant from METAvivor and by the U.S. Army Medical and Materiel Command Breast Cancer Idea Program, Grant W81WH-1s2-1-0127. We thank Dr. K. Sandeep Prabhu for thoughtful discussion.

Conflict of interest The authors declare that they have no conflict of interest.

References

1. DeSantis C et al (2013) Breast cancer statistics, 2013. Cancer J Clin 64(1):52–62
2. Klein CA (2011) Framework models of tumor dormancy from patient-derived observations. Curr Opin Genet Dev 21(1):42–49
3. Demicheli R et al (2007) Tumor dormancy and surgery-driven interruption of dormancy in breast cancer: learning from failures. Nat Clin Pract Oncol 4(12):699–710
4. Lipton A et al (2009) The science and practice of bone health in oncology: managing bone loss and metastasis in patients with solid tumors. J Natl Compr Cancer Netw 7(Suppl 7):S1–S29 quiz S30
5. Rubens RD (2000) Bone metastases–incidence and complications. In: Rubens RD, Mundy GR (eds) Cancer and the skeleton. Martin Dunitz, London 286
6. Naumov GN, Folkman J, Straume O (2009) Tumor dormancy due to failure of angiogenesis: role of the microenvironment. Clin Exp Metastasis 26(1):51–60
7. Demicheli R et al (2008) Recurrence dynamics does not depend on the recurrence site. Breast Cancer Res 10(5):R83
8. Aguirre-Ghiso JA, Bragado P, Sosa MS (2013) Metastasis awakening: targeting dormant cancer. Nat Med 19(3):276–277
9. Weiss L (1990) Metastatic inefficiency. Adv Cancer Res 54:159–211
10. Pantel K et al (1993) Differential expression of proliferation-associated molecules in individual micrometastatic carcinoma cells. J Natl Cancer Inst 85(17):1419–1424
11. Hedley BD, Chambers AF (2009) Tumor dormancy and metastasis. Adv Cancer Res 102:67–101
12. Takeuchi H, Muto Y, Tashiro H (2009) Clinicopathological characteristics of recurrence more than 10 years after surgery in patients with breast carcinoma. Anticancer Res 29(8):3445–3448
13. Pantel K et al (2003) Detection and clinical implications of early systemic tumor cell dissemination in breast cancer. Clin Cancer Res 9(17):6326–6334
14. Pantel K, Brakenhoff RH, Brandt B (2008) Detection, clinical relevance and specific biological properties of disseminating tumour cells. Nat Rev Cancer 8(5):329–340
15. Baccelli I et al (2013) Identification of a population of blood circulating tumor cells from breast cancer patients that initiates metastasis in a xenograft assay. Nat Biotechnol 31(6):539–544
16. Das Roy L et al (2009) Breast-cancer-associated metastasis is significantly increased in a model of autoimmune arthritis. Breast Cancer Res 11(4):R56
17. Yano S (2014) Metastatic bone lesion due to methotrexate and etanercept 24 years after breast cancer treatment. BMJ Case Rep. doi:10.1136/bcr-2013-202615
18. Rotolo N et al (2013) Metastasis at a tracheostomy site as the presenting sign of late recurrent breast cancer. Head Neck 35(11):E359–E362
19. Demicheli R et al (2008) The effects of surgery on tumor growth: a century of investigations. Ann Oncol 19(11):1821–1828
20. Schneider A et al (2005) Bone turnover mediates preferential localization of prostate cancer in the skeleton. Endocrinology 146(4):1727–1736
21. Tashjian AH Jr, Gagel RF (2006) Teriparatide [human PTH(1-34)]: 2.5 years of experience on the use and safety of the drug for the treatment of osteoporosis. J Bone Miner Res 21(3):354–365
22. Mundy GR et al (2008) Cytokines and bone remodeling. In: Marus R et al (eds) Osteoporosis. Editors Academic Press, New York, pp 491–528
23. Dhurjati R et al (2006) Extended-term culture of bone cells in a compartmentalized bioreactor. Tissue Eng 12(11):3045–3054
24. Cailleau R, Olive M, Cruciger QV (1978) Long-term human breast carcinoma cell lines of metastatic origin: preliminary characterization. In Vitro 14:911–915
25. Mastro AM, Vogler EA (2009) A three-dimensional osteogenic tissue model for the study of metastatic tumor cell interactions with bone. Cancer Res 69(10):4097
26. Phillips KK et al (1996) Suppression of MDA-MB-435 breast carcinoma cell metastasis following the introduction of human chromosome 11. Cancer Res 56(6):1222–1227
27. Krishnan V et al (2011) Dynamic interaction between breast cancer cells and osteoblastic tissue: comparison of two- and three-dimensional cultures. J Cell Physiol 226(8):2150–2158
28. Phadke PA et al (2008) BRMS1 suppresses breast cancer experimental metastasis to multiple organs by inhibiting several steps of the metastatic process. Am J Pathol 172(3):809–817
29. Sosnoski DM et al (2012) Changes in cytokines of the bone microenvironment during breast cancer metastasis. Int J Breast Cancer 2012:160265
30. Wang H et al (1997) Basic fibroblast growth factor causes growth arrest in MCF-7 human breast cancer cells while inducing both mitogenic and inhibitory G1 events. Cancer Res 57(9):1750–1757
31. Sato K et al (1986) Stimulation of prostaglandin E2 and bone resorption by recombinant human interleukin 1 alpha in fetal mouse bones. Biochem Biophys Res Commun 138(2):618–624
32. Sato K et al (1987) Tumor necrosis factor type alpha (cachectin) stimulates mouse osteoblast-like cells (MC3T3-E1) to produce macrophage-colony stimulating activity and prostaglandin E2. Biochem Biophys Res Commun 145(1):323–329
33. Bai X et al (2013) Prostaglandin E(2) receptor EP1-mediated phosphorylation of focal adhesion kinase enhances cell adhesion and migration in hepatocellular carcinoma cells. Int J Oncol 42(5):1833–1841
34. Sudo H et al (1983) In vitro differentiation and calcification in a new clonal osteogenic cell line derived from newborn mouse calvaria. J Cell Biol 96(1):191–198
35. Schneider CA, Rasband WS, Eliceiri KW (2012) NIH Image to ImageJ: 25 years of image analysis. Nat Methods 9(7):671–675
36. Pilbeam CC, Harrison JR, Raisz LG (2002) Prostaglandins and bone metabolism. In: Bilezikian JP, Raisz LG, Rodan GA (eds) Principles of bone biology. Academic Press, New York
37. Mundy GR et al (2001) Cytokines and bone remodeling. In: Marcus RE, Feldman D, Kelsey J (eds) Osteoporosis. Academic Press, New York, pp 373–403

38. Mark KS, Trickler WJ, Miller DW (2001) Tumor necrosis factor-alpha induces cyclooxygenase-2 expression and prostaglandin release in brain microvessel endothelial cells. J Pharmacol Exp Ther 297(3):1051–1058
39. Ono M (2008) Molecular links between tumor angiogenesis and inflammation: inflammatory stimuli of macrophages and cancer cells as targets for therapeutic strategy. Cancer Sci 99(8):1501–1506
40. Oshima H, Oshima M (2012) The inflammatory network in the gastrointestinal tumor microenvironment: lessons from mouse models. J Gastroenterol 47(2):97–106
41. Najmi S et al (2005) Flavopiridol blocks integrin-mediated survival in dormant breast cancer cells. Clin Cancer Res 11(5):2038–2046
42. Phadke PA, Mercer RR, Harms JF, Jia Y, Kappes JC, Frost AR, Jewell JL, Bussard KM, Nelson S, Moore C, Gay CV, Mastro AM, Welch DR (2006) Kinetics of metastatic breast cancer cell trafficking in bone. Clin Cancer Res 12:1431–1440
43. Blackwell KA, Raisz LG, Pilbeam CC (2010) Prostaglandins in bone: bad cop, good cop? Trends Endocrinol Metab 21(5):294–301
44. Ristimaki A et al (2002) Prognostic significance of elevated cyclooxygenase-2 expression in breast cancer. Cancer Res 62(3):632–635
45. Singh B et al (2007) COX-2 involvement in breast cancer metastasis to bone. Oncogene 26(26):3789–3796
46. Schrey MP, Patel KV (1995) Prostaglandin E2 production and metabolism in human breast cancer cells and breast fibroblasts. Regulation by inflammatory mediators. Br J Cancer 72(6):1412–1419
47. Cicek M et al (2005) Breast cancer metastasis suppressor 1 inhibits gene expression by targeting nuclear factor-kappaB activity. Cancer Res 65(9):3586–3595
48. Klein DC, Raisz LG (1970) Prostaglandins: stimulation of bone resorption in tissue culture. Endocrinology 86(6):1436–1440
49. Planchon P et al (1995) Evidence for separate mechanisms of antiproliferative action of indomethacin and prostaglandin on MCF-7 breast cancer cells. Life Sci 57(12):1233–1240
50. Sosa MS, Bragado P, Aguirre-Ghiso JA (2014) Mechanisms of disseminated cancer cell dormancy: an awakening field. Nat Rev Cancer 14(9):611–622
51. Wilson A, Trumpp A (2006) Bone-marrow haematopoietic-stem-cell niches. Nat Rev Immunol 6:93–106
52. Shiozawa Y et al (2008) The bone marrow niche: habitat to hematopoietic and mesenchymal stem cells, and unwitting host to molecular parasites. Leukemia 22(5):941–950
53. Mirza AA et al (2014) MEKK2 regulates focal adhesion stability and motility in invasive breast cancer cells. Biochim Biophys Acta 1843(5):945–954
54. Khoon MCS (2015) Experimental models of bone metastasis: opportunities for the study of cancer dormancy. Adv Deliv Rev. doi:10.1016/j.addr.2015.02.007

Journal of Cellular Physiology

In Vitro Mimics of Bone Remodeling and the Vicious Cycle of Cancer in Bone

VENKATESH KRISHNAN,[1,2] ERWIN A. VOGLER,[3,4,5] DONNA M. SOSNOSKI,[1] AND ANDREA M. MASTRO[1]*

[1]*Department of Biochemistry and Molecular Biology, The Pennsylvania State University, University Park, Pennsylvania*

[2]*The Huck Institutes of Life Sciences, The Pennsylvania State University, University Park, Pennsylvania*

[3]*Department of Materials Science and Engineering, The Pennsylvania State University, University Park, Pennsylvania*

[4]*Department of Bioengineering, The Pennsylvania State University, University Park, Pennsylvania*

[5]*Materials Research Institute, The Pennsylvania State University, University Park, Pennsylvania*

Bone remodeling is a natural process that enables growth and maintenance of the skeleton. It involves the deposition of mineralized matrix by osteoblasts and resorption by osteoclasts. Several cancers that metastasize to bone negatively perturb the remodeling process through a series of interactions with osteoclasts, and osteoblasts. These interactions have been described as the "vicious cycle" of cancer metastasis in bone. Due to the inaccessibility of the skeletal tissue, it is difficult to study this system in vivo. In contrast, standard tissue culture lacks sufficient complexity. We have developed a specialized three-dimensional culture system that permits growth of a non-vascularized, multiple-cell-layer of mineralized osteoblastic tissue from pre-osteoblasts. In this study, the essential properties of bone remodeling were created in vitro by co-culturing the mineralized collagenous osteoblastic tissue with actively resorbing osteoclasts followed by reinfusion with proliferating pre-osteoblasts. Cell–cell and cell–matrix interactions were determined by confocal microscopy as well as by assays for cell specific cytokines and growth factors. Osteoclasts, differentiated in the presence of osteoblasts, led to degradation of the collagen-rich extracellular matrix. Further addition of metastatic breast cancer cells to the co-culture mimicked the vicious cycle; there was a further reduction in osteoblastic tissue thickness, an increase in osteoclastogenesis, chemotaxis of cancer cells to osteoclasts and formation of cancer cells into large colonies. The resulting model system permits detailed study of fundamental osteobiological and osteopathological processes in a manner that will enhance development of therapeutic interventions to skeletal diseases.

J. Cell. Physiol. 229: 453–462, 2014.

Metastatic cancer in bone is effectively an incurable disease (Woodhouse et al., 1997; Rubens, 1998; Rubens and Mundy, 2000) that progresses with significant morbidity related to massive bone loss or gain, bone pain, hypercalcemia, pathological fractures, and spinal cord compression (Nielsen et al., 1991). Approximately 25% of breast cancers metastasize, with bone as the first site of metastasis in 46% of cases and over 70% of cases in patients with first relapse (Landis et al., 1999). Statistics for prostate cancer and myeloma are equally compelling (Logothetis and Lin, 2005).

Cancer, once metastasized to the skeleton, disrupts the balance between bone formation and resorption. Ultimately, the structural integrity of the bone is impaired either by bone degradation due to osteoclastic activity (common in breast cancer metastasis) or by excess bone formation due to increased ostoblastic activity (common in prostate cancer). Cytokines and other factors produced by both tumor and bone cells interact through a process that has been described as a "vicious cycle" of bone metastasis. Factors released from the bone matrix fuel breast cancer proliferation, which leads to yet more bone loss or production (Guise and Mundy, 1998; Rubens and Mundy, 2000). There are currently no in vitro models to study the bone-remodeling process, especially one that incorporates cancer cells.

The extensiveness of the skeleton, opacity of bone, and difficulty accessing the bone marrow cavity in the clinic undoubtedly account for the fact that metastases and osteolytic lesions are usually detected late in the metastatic process. Accessibility is also a problem that hinders a full appreciation of the cellular and molecular mechanisms involved in early-stage cancer colonization of bone. This problem hampers development of therapeutic interventions. Although excised tissue faithfully captures the end stages of bone metastasis associated with fully developed tumors, critical

Venkatesh Krishnan's present address is Department of Surgery, Section of Urology, The University of Chicago, Chicago, IL

The authors declare that there are no conflicts of interest.

Contract grant sponsor: US Army Medical and Materiel Research Command Breast Cancer program;
Contract grant number: WX81XWH-06-1-0432.
Contract grant sponsor: Susan G Komen Breast Cancer Foundation;
Contract grant number: BCTR 0601044.
Contract grant sponsor: Penn State Hershey Cancer Institute.

*Correspondence to: Andrea M. Mastro, Professor of Microbiology and Cell Biology, Department of Biochemistry and Molecular Biology, 308 Althouse Laboratory, The Pennsylvania State University, University Park, PA 16802.
E-mail: a36@psu.edu

Manuscript Received 9 November 2012
Manuscript Accepted 27 August 2013

Accepted manuscript online in Wiley Online Library (wileyonlinelibrary.com): 11 September 2013.
DOI: 10.1002/jcp.24464

initial stages of this process remain substantially inaccessible (Welch, 1997). Thus, there is an urgent need for clinically relevant experimental models suitable for the study of bone metastases that will catalyze development of new therapeutic interventions.

Development of in vitro bone-tissue models and bone-remodeling mimics has proven to be a significant challenge in the fields of bone biology and tissue engineering, partly because of the complexity of bone and partly because of the long time frames over which bone cells mature to carry out important physiological functions. To create a model that can faithfully mimic the pathophysiology of bone metastatic cancer, it is important to maintain and recreate the characteristic 3D architecture of the tissue under investigation. Specifically, to study the interaction of metastatic cells with the secondary tissue microenvironment requires a system adept in handling not only the complexity of the host tissue but one that also allows the study of the cancer cell interaction with the host tissue. In vivo, cells function within the context of a highly specialized microenvironment that is specific to the cell type and the anatomical location. Culture of cells in vitro using standard two-dimensional (2D) monolayer techniques limits their physiological context and impacts cellular function. Some major limitations of a 2D culture are the lack of structural architecture, and the inefficient mobilization of nutrients and removal of waste metabolites over the long term. The fundamental requirements of a 3D model are the support of growth and co-culture of different cell types, the efficient exchange of cytokines and growth factors (for an autocrine and paracrine effect), production of an extra-cellular matrix (ECM) as necessary 3D scaffolding for mechanical stability and for regulating cellular functions (Kim, 2005). Depending on the type of 3D system, the culture offers rapid and meaningful experimental manipulations and permits real-time monitoring of cell–cell and cell–matrix interactions. With the advancement of tissue engineering strategies, several successful 3D models have been implemented (Griffith and Naughton, 2002; Kim, 2005). One commonly used approach is culture of organ explants. These whole organ or tissues retain their 3D architecture and cellular complexity in vitro. This technique has been mainly used for short-term cultures of otherwise hard to grow tissues such as brain and embryonic glands (Gahwiler et al., 1997; Sakai et al., 2003). Nordstrand et al. (2009) implemented a murine calvarial explant to study the interaction of prostate cancer cell with bone microenvironment. They used a two-compartment co-culturing system to study prostate cancer-induced bone remodeling. The primary concern with organ culture is that it may not permit adequate oxygenation and allow tissue necrosis. However, studies of tumor biology have benefited from the hypoxia setting which mimics the nutrient and oxygen insufficiency at the tumor-host interaction (Hicks et al., 2006). Curtin et al. (2012) utilized a (3D) cancer-bone metastasis model composed of free-floating live mouse calvarial bone organs in the presence of cancer cells in a roller tube system. This system simulates the in vivo bone tissue under defined conditions at specific bone remodeling stages. It was possible to induce hypoxic conditions experienced by both bone microenvironment and solid tumors. Even with advancement in ex vivo culturing of cells and tissues using the 3D models, there are limitations. Few models go beyond culturing more than two cell types in one system. For example, the interaction of mineralized bone cells and cancers such as breast and prostate has been advanced using 3D scaffolds established from cell lines, dissociated tumor cells or stem cells (Smalley et al., 2006). Cells are typically grown in standard tissue culture and implanted into a 3D matrix-scaffold either as single cells or tissue aggregates. The scaffolds can range from biodegradable polymers to type I collagen or matrix derived from native extracellular matrix following decellularization. Papadimitropoulos et al., presents a physiologically complex 3D model that encapsulates a tri-culture of osteoblasts and osteoclasts and endothelial cells. This multi-cell culture system was shown to form ectopic bone-like tissue with functional osteoblasts and osteoclasts (Papadimitropoulos et al., 2011). However, a bone-remodeling mimic requires a supplement of fresh pre-osteoblasts providing the potential for differentiation into cells necessary for the repair of bone-like tissue. Furthermore, to study a disease process such as cancer colonization of a secondary tissue, aforesaid designs appear to be limited in representing a complex heterologous multicellular tumor model. Nevertheless, these efforts are a step closer to a physiologically relevant organotypic model.

For improved understanding of breast cancer colonization of bone, we have taken in vitro culture a step further and overcome some of these issues. Our specialized culture method permits the aim of this study was to determine whether 3D mineralizing tissue derived from the co-culture of osteoblasts with osteoclasts in a novel bioreactor would be a relevant in vitro bone surrogate for studying the early stages of breast cancer colonization. We show that addition of osteolytic cancer cells upsets bone remodeling in vitro in a manner consistent with the vicious cycle of metastatic cancer colonization in bone.

Materials and Methods

Culture methods

Cell culture was performed in specialized bioreactors based on the principle of simultaneous growth and dialysis implemented as described previously (Dhurjati et al., 2006, 2008; Krishnan et al., 2010, 2011). Briefly, the bioreactor design (Supplementary Fig. 1) separates a cell growth compartment (5 ml) and a medium reservoir (30 ml) by a dialysis membrane with a 6–8 kDa cut-off. Cells were inoculated into the growth chamber in complete medium including serum, and grown directly on the bottom gas-permeable film. The reservoir was filled with basal medium without serum. Serum constituents or macromolecules synthesized by cells with molecular weights in excess of the dialysis membrane cutoff (6–8 kDa) were retained and concentrated within the growth compartment. Low molecular weight metabolic waste products such as lactic acid continuously dialyzed out of the growth space into the media reservoir against a concentration gradient created by the 6:1 volume ratio and periodic refreshment of the reservoir medium (without perturbing the growth compartment pericellular environment). Conversely, low-molecular weight nutrients such as hexose and amino acids dialyzed from the reservoir into the growth space against a concentration gradient created by the volume ratio and metabolic demand of cells within the growth space. At the end of culture periods, bioreactors were dismantled, and tissue formed on the bottom film was cut into pieces for various biochemical assays. Supernatants from both chambers were collected and stored at −80°C for ELISA.

Murine pre-osteoblasts (MC3T3-E1), a gift from Dr. Norman Karin, Pacific Northwest National Laboratories, were inoculated into the growth chamber of the bioreactor (10^4 cells/cm^2) and cultured with alpha minimum essential medium (α-MEM, Mediatech, Herdon, VA), 10% neonatal FBS (Cansera, Roxdale, Ontario), 100 U/ml penicillin, 100 μg/ml streptomycin (Sigma–Aldrich, St. Louis, MO). The reservoir contained the same medium but without serum. Bioreactors were maintained at 37°C in a humidified, 5% CO_2 incubator. Once the cells reached confluence, usually 4–5 days, the medium in the growth chamber was replaced with differentiation medium containing 50 μg/ml ascorbic acid and 10 mM β-glycerophosphate (Sigma–Aldrich). Basal medium within the medium reservoir was replaced every 30 days to prevent the accumulation of metabolic wastes. Osteoblast cultures were

maintained for 60 days prior to the start of co-cultures and tri-cultures.

Osteoclasts were obtained from bone marrow cells harvested from 6 to 9 weeks old GFP (Tg(CAG-EGFP)B5 Nagy J mice and/or dsRED mice with approval from the Penn State University Institutional Animal Care and Use committee. Femurs were flushed with a 26-gauge needle with α-MEM, 100 U/ml penicillin, and 100 μg/ml streptomycin. Cells from two femurs were pooled together and cultured for 24 h at 37°C in a T-150 culture flask in α-MEM, 10% neonatal FBS, 100 U/ml penicillin, 100 μg/ml streptomycin. Pre-osteoclasts were enriched by collecting the non-adherent cells after the 24 h incubation. These non-adherent marrow-derived cells were inoculated at 3×10^4 cells/cm^2 in medium supplemented with 50 ng/ml RANKL (gift from AMGEN®, Thousand Oaks, CA) and 100 ng/ml M-CSF (Peprotech, Rockyhill, NJ) into a bioreactor containing osteoblast tissue that had been grown for 60 days. Pre-osteoclasts were co-cultured with osteoblast tissue for 21 days.

Tri-cultures of osteogenic tissue, osteoclasts, and metastatic breast cancer cells were created by inoculation of co-cultures with MDA-MB-231-GFP breast cancer cells (gift from Dr. Danny Welch from University of Kansas Cancer Center) at 10^3 cells/cm^2. Pre-osteoclasts were cultured on 60-day-old osteoblasts for 10 days. Next, MDA-MB-231-GFP cells were introduced and cultured for an additional 10 days. With the addition of osteoclasts (co-culture) and breast cancer cells (tri-culture), the media from the top chamber was completely refreshed once every 7 days with fresh basal media.

Biochemical and immunochemical assays

Staining for cell morphology and collagen. Tissue samples from the bioreactors were harvested and fixed in 4% paraformaldehyde in PBS buffer. For visualization of cell morphology, samples were stained for actin filaments with AlexaFluor 568-phalloidin (Molecular Probes, Invitrogen Corporation, Carlsbad, CA). For collagen detection, samples were immunolabeled with an anti-collagen Type I antibody (LF 41, gift from Dr. Larry Fisher, NIH) at a 1:100 dilution in PBS 1% goat serum overnight at 4°C. Goat anti-rabbit antibodies, AlexaFluor 647 (Invitrogen) at a dilution of 1:200 in PBS 1% goat serum were used for detection. Images were collected by sequential scans using the Olympus FV300 laser scanning confocal microscope. The Z-sections were 3D-reconstructed using AutoQuant v9.3 software.

Tartrate resistant acid phosphatase (TRAP) staining. Tissue samples were fixed in 4% paraformaldehyde and stained for TRAP using the Leukocyte Acid Phosphatase Kit (Sigma–Aldrich) following the manufacturer's protocol.

C-telopeptide assay. Supernatants collected from bioreactors at the end of each culture period were assayed with an ELISA kit for C-terminal telopeptides (CTX; Immunodiagnostic Systems, Inc., Fountain Hills, AZ).

Cytokine analysis. Supernatants collected at the end of culture periods were assayed for KC and MIP-2 with a Milliplex 5-plex mouse cytokine array (Millipore Corporation, Billerica, MA). IL-6 levels were determined by standard sandwich ELISA technique using murine-specific antibodies (R&D Systems, Minneapolis, MN).

Gene expression

Total RNA was extracted from bioreactor cultures using the RNeasy kit (Qiagen, Valencia, CA) with on-column DNase treatment. First strand cDNA synthesis was performed using the Qscript cDNA kit (Quanta Biosciences, Gaithersburg, MD). The gene expression was determined by real-time quantitative PCR using the ABI Prism 7000 sequence detection system (Applied Biosystems, Carlsbad, CA) and SYBR Green (Quanta Biosciences). Primers were designed to specifically target mouse gene sequences (Supplementary Table 1). A standard curve was generated for each gene transcript using fivefold serial dilutions of cDNA prepared from either MC3T3-E1 (for osteoblast transcripts) or mouse bone marrow cells (for osteoclast and GFP transcripts). Relative expression levels were normalized to levels of mouse GAPDH and derived from the standard curve for each gene transcript. For the analysis of transcripts from cultures that contained both mouse osteoblast and osteoclasts, the levels were again normalized by determining the percentage of RNA derived from the osteoblasts (which contain no GFP transcripts) and from the mouse bone marrow cells (which express GFP). These percentages were derived from a standard curve containing known amounts of osteoblast and GFP mouse bone marrow cells. Thus, all results shown are corrected for total mouse RNA and osteoblast/bone marrow cell content.

Statistical analyses

Data were analyzed by two-tailed paired *t*-test using the GraphPad Prism Software, Inc. Reported *P*-values are $^*<0.05$, $^{**}<0.001$, and $^{***}<0.0001$.

Results

Bone remodeling in vitro

MC3T3-E1, murine calvarial pre-osteoblasts, were grown for 60 days (2 months) in the bioreactor to form a 3D, collagenous osteoblastic tissue. After fixation and staining with phalloidin, cuboidal osteoblast cells (Fig. 1A) appeared to be enmeshed in thick ECM composed largely of collagen (Fig. 1B,C, Supplementary Fig. 2). The 2-month-old osteoblastic tissue was used as the standard tissue for all co-culture and tri-culture experiments.

In order to determine if osteoclasts could be cultured under the same conditions, cells derived from bone marrow of GFP mice were cultured in medium supplemented with RANKL and M-CSF for 21 days. This procedure resulted in the formation of multinucleated giant osteoclast-like cells (Fig. 1D). Co-culture of non-adherent bone marrow cells on the 60 day osteoblast tissue produced multinucleated mature TRAP positive osteoclasts (Fig. 1E, inset) that migrated on osteoblast-derived tissue (Fig. 1E). These osteoclasts actively digested collagenous osteogenic tissue (compare Fig. 1C–F), and aggregated into nest-like structures in the presence of mature osteoblasts (Fig. 1G) reminiscent of osteoclast resorption of authentic bone and formation of resorption pits.

We expanded this model by adding pre-osteoblasts to mimic the bone-building phase of the remodeling process. Subsequent infusion of this osteoblast/osteoclast co-culture with pre-osteoblasts led to refilling of the resorbed matrix with a confluent layer of osteoblasts over 7 days of observation (Fig. 1H,I). There was a commensurate increase in the collagen matrix thickness. To further characterize the extent of resorption and rebuilding, we performed a Z-scan on the three tissues. (Fig. 1C,F,I are 3D reconstruction of Z stacks from tissues shown in B,G,H). When a 22 μm thick osteoblast tissue (Fig. 1C) was co-cultured with osteoclasts, there was a 1.6-fold reduction in tissue thickness (Fig. 1F, 13.5 μm) and loss of collagen. Addition of new pre-osteoblasts brought about repair of the osteoblast/osteoclast tissue with a final tissue thickness of 24 μm (Fig. 1I).

Gene expression patterns in an in vitro bone remodeling unit

Gene expression profiles of characteristic osteoblast and osteoclast proteins were consistent with osteoblastic tissue resorption and replacement (Fig. 2). Alkaline phosphatase expression was readily detected in cultures containing only osteoblasts (Fig. 2A). Upon addition of osteoclasts there was a

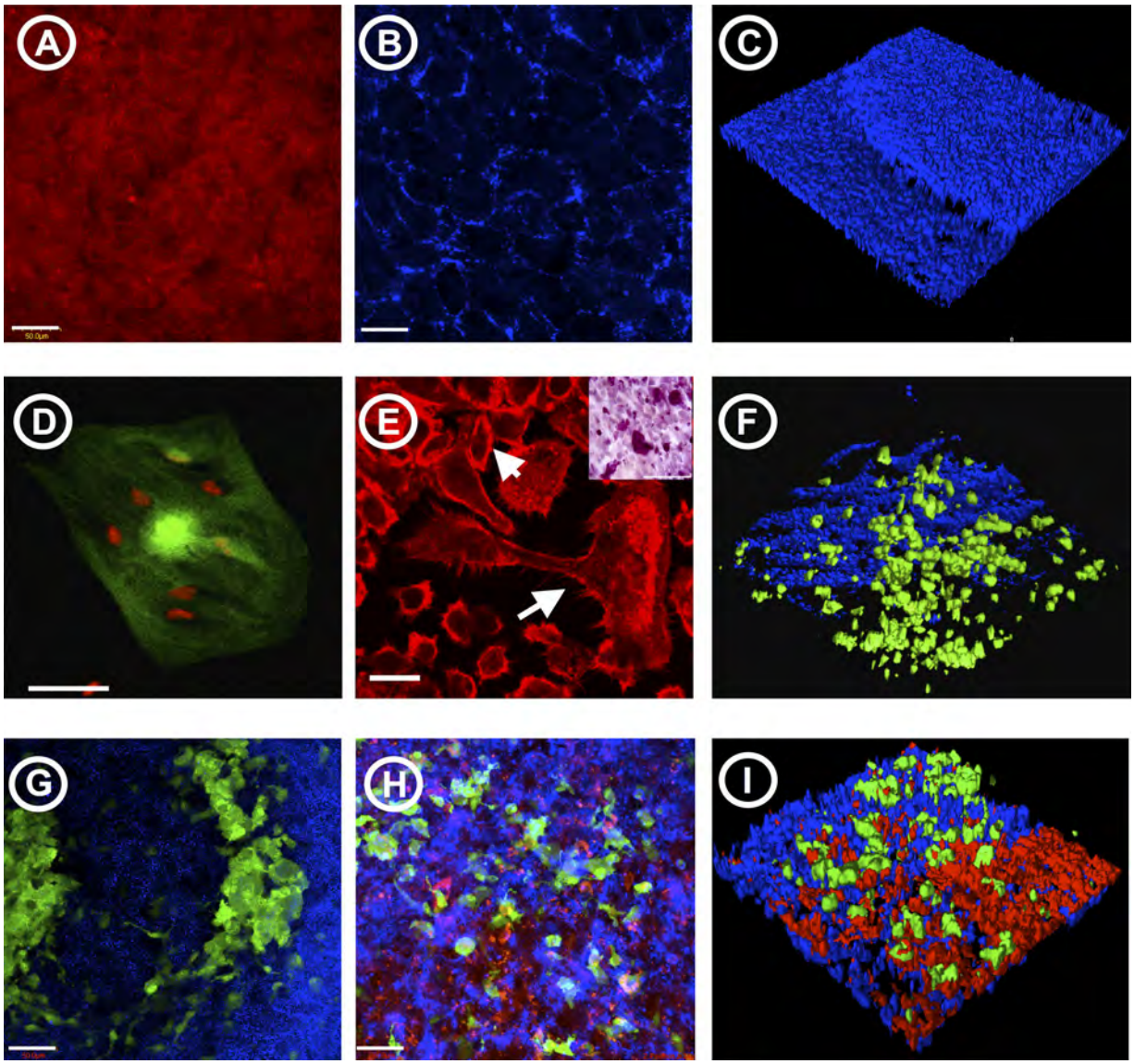

Fig. 1. A bone-remodeling mimic. A: MC3T3-E1 osteoblastic tissue after 60 days of continuous culture using a specialized culture method. Shown are fluorescent, phalloidin-stained, actin fibers of osteoblasts. B: Immunostaining of type I collagen resolving fibrillar formations (blue) surrounding dark osteoblasts. C: Confocal reconstruction of immunostained collagen (blue) reveals a 22 μm thick ECM. D: A multinucleated GFP-osteoclast with five prominent red stained (Draq 5) nuclei derived from osteoclast precursors. Osteoclasts were cultured for 3 weeks with 60 day osteoblastic tissue. E: An actin stained osteoclast (arrow) migrating on the osteogenic tissue in the presence of osteoblasts (arrowheads). Inset shows a TRAP positive multinucleated osteoclast on osteoblast tissue counter-stained with eosin. F: Confocal reconstruction of GFP-osteoclasts in the presence of collagen (blue). Matrix degradation by osteoclasts resulted in a net decrease in tissue thickness from 22 to 13.5 μm. G: GFP-osteoclasts assembled into nest-like structures within blue stained ECM after 3 weeks of co-culture. H: MC3T3-E1 pre-osteoblasts were vital stained (red) and infused into a co-culture of osteoblasts (unstained) and osteoclasts (green). They proliferated within the ECM (blue) after 7 days. I: Confocal reconstruction showed that red osteoblasts filled regions of digested ECM, and restored tissue thickness to 24 μm. Scale bars: A, B, G, and H are 50 μm. D, and E are 20 μm.

significant (2.5-fold) downregulation of alkaline phosphatase. The inoculation of fresh osteoblasts did not result in a complete recovery of alkaline phosphatase likely due to the fact that these cells were cultured for only one additional week (Fig. 2A). The expression of osteocalcin, a marker of osteoblast mineralization was reduced by 2.2-fold in the presence of osteoclasts (Fig. 2B). A recovery (twofold) of osteocalcin expression was observed when the pre-osteoblasts were added to the culture (Fig. 2B). This trend was also seen in the protein levels of osteocalcin (data not shown). Type I collagen, the major constituent of the bone extracellular matrix was significantly reduced (12.5-fold) in the presence of osteoclasts with a 7.5-fold reversal of the expression upon addition of fresh osteoblasts (Fig. 2C). We did not detect any TRAP activity in bioreactors with osteoblasts only (Fig. 2D). The osteoblast–osteoclast co-culture had a 1.5-fold increase in the expression of TRAP that subsequently appeared to be downregulated in the presence of additional fresh osteoblasts (Fig. 2D). The

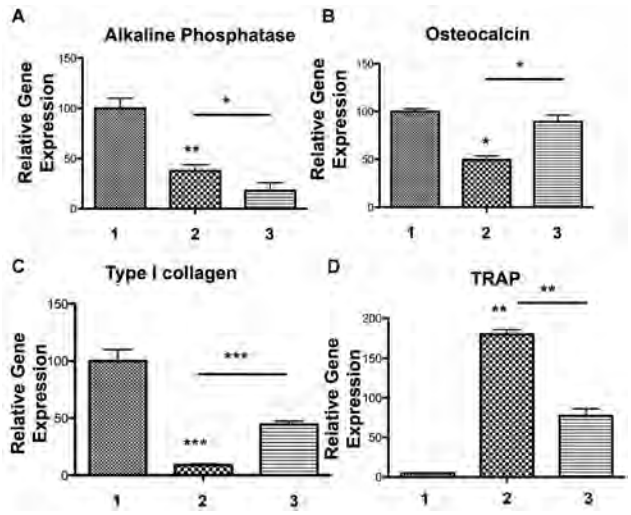

Fig. 2. Gene expression changes during bone remodeling in vitro. Gene expression analysis was performed by real-time quantitative PCR using the ABI Prism 7000 sequence detection system (Applied Biosystems) and SYBR Green (Quanta Biosciences). Primers designed for GFP were used to determine the cell type, the ratio of osteoblasts and osteoclasts. GAPDH served as the internal control. Relative transcript levels were calculated from the relative standard curve generated using stock cDNA dilutions and normalized to the internal control. Osteoblast gene expression is plotted in (A) alkaline phosphatase, (B) osteocalcin, (C) type I collagen. Osteoclast gene expression is plotted in (D) tartrate resistant acid phosphatase, TRAP. Sample size, n = 3. Unless indicated with a bar, statistical significances are in relation to cultures with only osteoblasts (1). Significance was determined as $^{*}P$-value < 0.05, $^{**}P$-value < 0.001, $^{***}P$-value < 0.0001. 1 = osteoblasts, 2 = osteoblast + osteoclasts, 3 = osteoblasts + osteoclasts + fresh osteoblasts.

increase in TRAP expression occurred with a concomitant decrease in osteoprotegerin, a decoy RANKL receptor (data not shown). Thus, co-culture of osteoblastic tissue with active osteoclasts followed by reinfusion of pre-osteoblasts mimicked the classical steps of bone remodeling.

Addition of breast cancer cells to a bone remodeling system in vitro

Introduction of MDA-MB-231 metastatic breast cancer cells into the osteoblast/osteoclast co-culture created a tri-culture consisting of the major cellular participants in the vicious cycle of metastatic cancer in bone (Fig. 3; Parts A,B,C in Fig. 3 are composite images of Z-stacks collected by confocal microscopy and the lower parts D,E,F are 3D reconstruction of the Z stacks to show the depth of the tissue). The 24 μm thick, 60 day osteoblast tissue (Fig. 3A,D), was reduced to a 16.5 μm thick tissue (Fig. 3B,E) after co-culture with osteoclasts for 3 weeks. Upon addition of breast cancer cells, the final tissue thickness was further reduced to 14.5 μm (Fig. 3C,F). Confocal 3D reconstructions of differentially stained osteoclasts, breast cancer cells, and collagen showed that breast cancer cells penetrated the osteoblastic tissue and formed cancer-osteoclast aggregates (Fig. 3F). To illustrate the effect of osteoclast-breast cancer on the osteoblast tissue, a tri-culture experiment with osteoblasts (unstained), osteoclasts (green) and breast cancer cells (bright green/yellow) was carried out. In the first day of tri-culture, breast cancer cells (arrows, Fig. 3G) migrated toward osteoclasts (circle Fig. 3G), eventually encircling foci of active osteoclasts (Fig. 3H, circle). At the end of the tri-culture period, cancer cells were observed to proliferate around areas of active resorption and formed a distinct colony that comprised of cancer cells, osteoclasts and pre-osteoclasts on the osteoblast tissue (Fig. 3I). The aggregate of these cells together degraded the osteoblast tissue that resulted in a resorption pit-like structure (Fig. 3I, inset).

Effect of breast cancer cells on the bone remodeling system in vitro

Osteoclastogenesis and corresponding gene expression profiles were consistent with the expectations of the vicious cycle of breast cancer in bone (Fig. 4). More osteoclasts differentiated in the presence of breast cancer cells than in the absence of cancer cells (Fig. 4A,C). Collagen was significantly degraded in the presence of osteoclasts compared to collagen from osteoblast-only cultures. However, we did not observe a change in the levels of C-telopeptide (a collagenase cleavage fragment) in the cultures that had breast cancer cells even though there was a 3.3-fold increase in TRAP positive osteoclasts in these cultures (Fig. 4B). Concomitant with the increase in the number of osteoclasts in the tri-culture (Fig. 4A), there was a significant increase in TRAP expression in the presence of breast cancer cells (Fig. 4C).

Osteoblast differentiation (i.e., osteocalcin expression) was downregulated in the presence of osteoclasts and cancer cells (Fig. 4D). In addition, collagen levels were measured by calculating the pixel density on the Z-stack of confocal images. There was a significant reduction in the levels of collagen density in the presence of osteoclasts and with breast cancer cells (Fig. 4E). However, the addition of breast cancer cells did not lead to further reduction of collagen levels.

Inflammatory response of bone remodeling unit in the presence of cancer cells

The murine GRO-α homologue, Keratinocyte Chemoattractant (KC), murine IL-8 homologue, Macrophage Inflammatory Protein-2 (MIP-2), and inflammatory cytokine IL-6 were analyzed. The three cytokines were not detected in cultures with osteoblasts alone (Fig. 5A,B,C, column 1). With the introduction of osteoclasts, there was a greater than twofold increase in both MIP-2 and KC (Fig. 5A,B, column 2). The levels were maintained in the tri-culture containing breast cancer cells (Fig. 5A,B, column 3). Addition of osteoclasts to osteoblasts did not result in an IL-6 response. However, introduction of breast cancer cells to the osteoblast–osteoclast co-culture resulted in a significant (twofold) increase in IL-6 levels (Fig. 5C, column B).

Discussion

Cancer metastasis is a multi-step process that starts with the shedding of neoplastic cells from the primary tumor and ends with formation of a secondary tumor in a host tissue (Liotta and Hart, 1982; Gabbert, 1985; Woodhouse et al., 1997; Bischoff et al., 2005). In the case of breast cancer, cells readily metastasize to areas of active bone growth such as the ends of long bones, sternum, and vertebrae (Phadke et al., 2006). Breast cancer cells preferentially collect in the metaphysis region lying between the epiphysis and the diaphysis (bone shaft) through a process possibly mediated by a pattern of lower blood flow and higher growth factor/cytokine concentrations. Cytokines produced by both tumor and bone cells set up what has been described as a "vicious cycle" of bone breakdown (Guise and Mundy, 1998) in which factors released from the bone matrix fuel breast cancer proliferation, which leads to yet more bone loss.

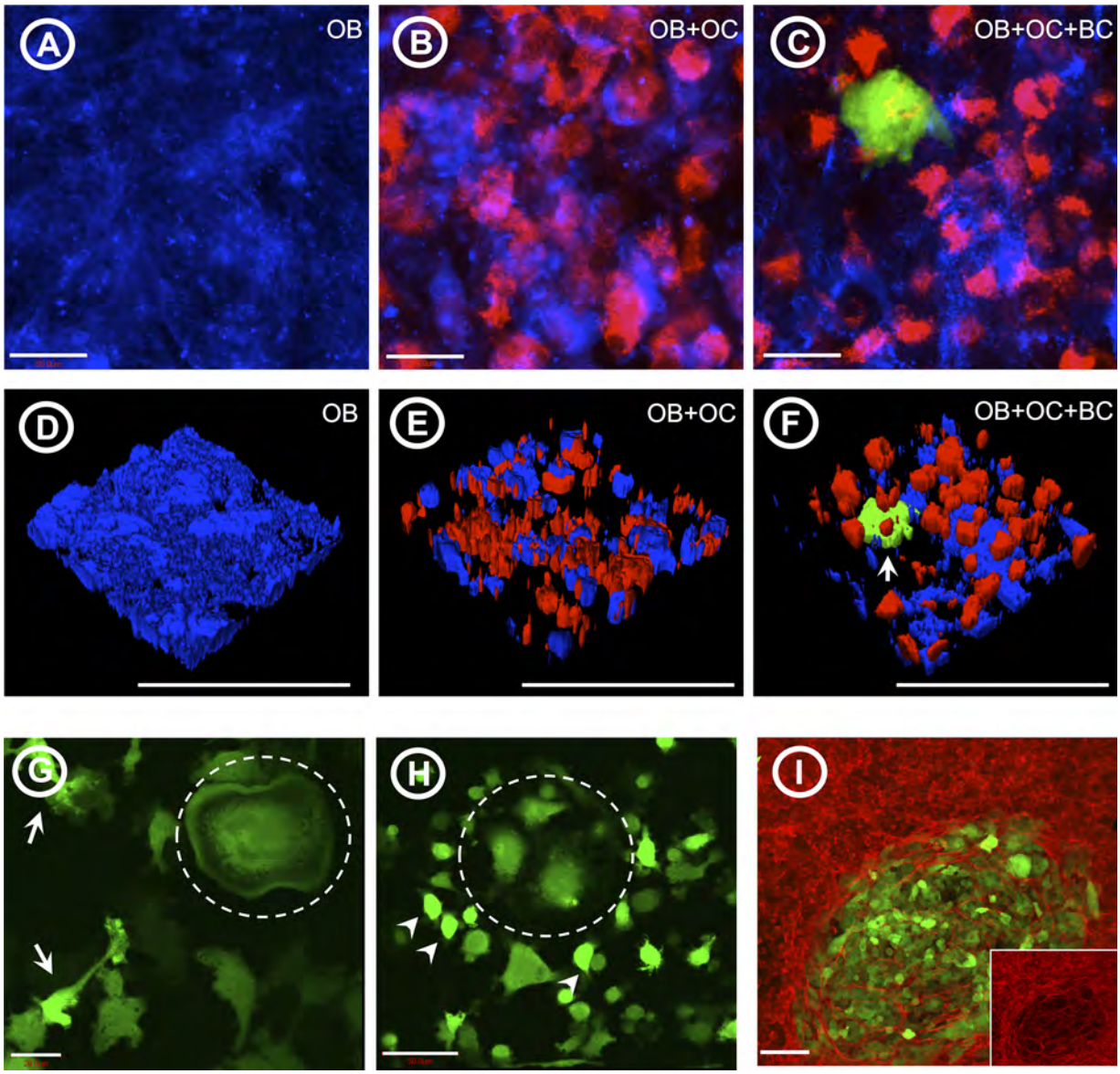

Fig. 3. A vicious cycle mimic. MC3T3-E1 cultured for 2 months (A,D) were co-cultured with non-adherent bone marrow cells from dsRED mice enriched for pre-osteoclasts and supplemented with RANKL (50 ng/ml) and MCSF (100 ng/ml) for 3 weeks (B,E). Metastatic breast cancer cells, MDA-MB-231-GFP, were added to the osteoblast–osteoclast co-culture to create a tri-culture system at the 10 day interval and cultured for an additional 10 days (C,F). At the end of culture periods, tissue samples were fixed in 4% para-formaldehyde and stained for type I collagen (blue) with an antibody as described in the methods. Stained samples were imaged with laser scanning confocal microscopy. A, B, and C are composite images of Z-stacks. D, E, and F are 3D reconstruction of A, B, and C, respectively, to show the depth of the tissue. A,D: Type I collagen made by 2-month-old MC3T3-E1 cultured in the bioreactor has a matrix thickness of approximately ~24 μm. B,E: A reduction of collagen thickness to 16.5 μm from 24 μm was seen upon co-culture with osteoclasts (red). C,F: Addition of breast cancer cells (green) to osteoblast–osteoclast (red) co-cultures resulted in the aggregation of cancer cells and osteoclasts to collectively further degrade the osteoblast matrix. The matrix thickness was reduced to 14.5 μm. Confocal reconstruction revealed that cancer cell colonies (green, arrow) in combination with osteoclasts (red) migrated to the bottom of the osteoblastic tissue. Shown are representative images from three bioreactors. (G) and (H) are live confocal images showing MDA-MB-231-GFP breast cancer cells' (arrows) migration towards GFP osteoclasts (dotted circles) in tri-cultures created by adding breast cancer cells to osteoblast–osteoclast. I: Breast cancer cells and osteoclasts congregated in nest-like structures formed in phalloidin-stained osteoblastic tissue 10 days after addition of cancer cells to the osteoblast–osteoclast co-culture (inset shows osteoblasts only). Scale bars for A, B, and C indicate 50 μm. D, E, and F indicate 150 μm. G = 20 μm, H = 50 μm, and I = 100 μm. OB, osteoblasts; OC, osteoclasts; and BC, breast cancer cells.

Given the complexity of the bone microenvironment, the process of cancer cell colonization of the bone should be studied at the organ level. However, whole-animal physiology can obscure details of the metastatic process, especially when the target, for example, bone, is difficult to access. (Mastro et al., 2003).

In principle, a sub-set of the metastatic process can be studied in vitro if the model system under consideration retains sufficient biological complexity to be a reasonable surrogate for host tissue. Effective in vitro models must strike a balance between experimental efficacy and retention of biological complexity. Three-dimensional tissue models have become a

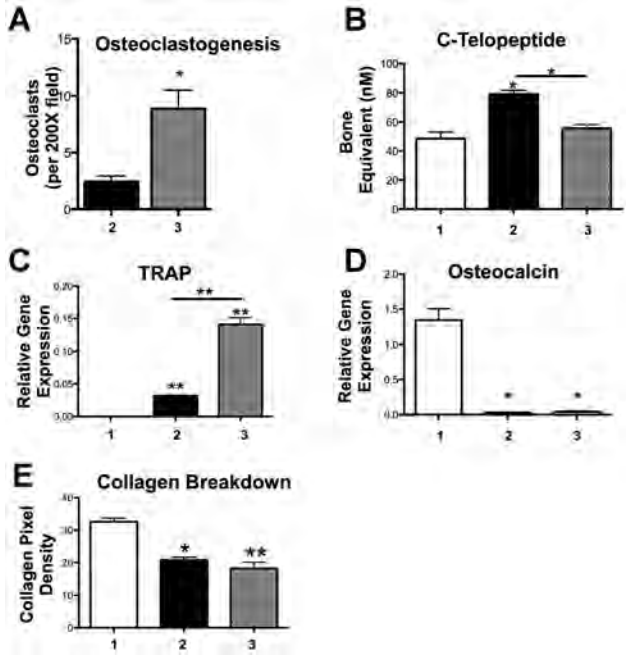

Fig. 4. Effect of breast cancer cells on the bone remodeling system in vitro. A: Ostoclastogenesis in the presence of breast cancer cells. Non-adherent bone marrow cells were added to bioreactors containing 2 month osteoblasts as described in the legend to Figure 1. To a cohort of co-cultures MDA-MB-231 cells were added. After 3 weeks, osteoclasts were stained for TRAP enzyme and fields picked at random were counted for TRAP positive cells containing three or more nuclei. The counts are from two separate bioreactors. Fifty fields of each bioreactor containing osteoblasts and osteoclasts were counted and 20 fields of each bioreactor containing osteoblasts, osteoclasts, and breast cancer cells were counted. B: Culture supernatants from co-cultures and tri-cultures were assayed for C-telopeptide (collagen breakdown product) by ELISA. Sample sizes for osteoblasts and osteoblasts, osteoclasts and breast cancer cells were three; sample sizes for osteoblasts and osteoclasts were two. C,D: For all three conditions, RNA was extracted and RT-PCR was carried out with primers specific to mouse species. Expression levels were normalized to an internal control of GAPDH and reported as relative gene expression to GAPDH. C: TRAP was analyzed as osteoclast activity, and osteocalcin (D) was analyzed as osteoblast activity. E: Collagen degradation was assessed for the three conditions by quantifying collagen pixel density from immunostained (for type I collagen) cultures. Collagen pixel density was calculated using Image J (NIH) from confocal Z-stacks that were collected from the different culture. Error bars represent three different randomly chosen areas from a bioreactor membrane. Similar trends were observed in two different bioreactors. Unless indicated with a bar, statistical significances are in relation to cultures with only osteoblasts. Significance was determined by $^{*}P$-value < 0.05, $^{**}P$-value < 0.001, $^{***}P$-value < 0.0001. 1 = osteoblasts, 2 = osteoblast + osteoclasts, 3 = osteoblasts + osteoclasts + breast cancer cells.

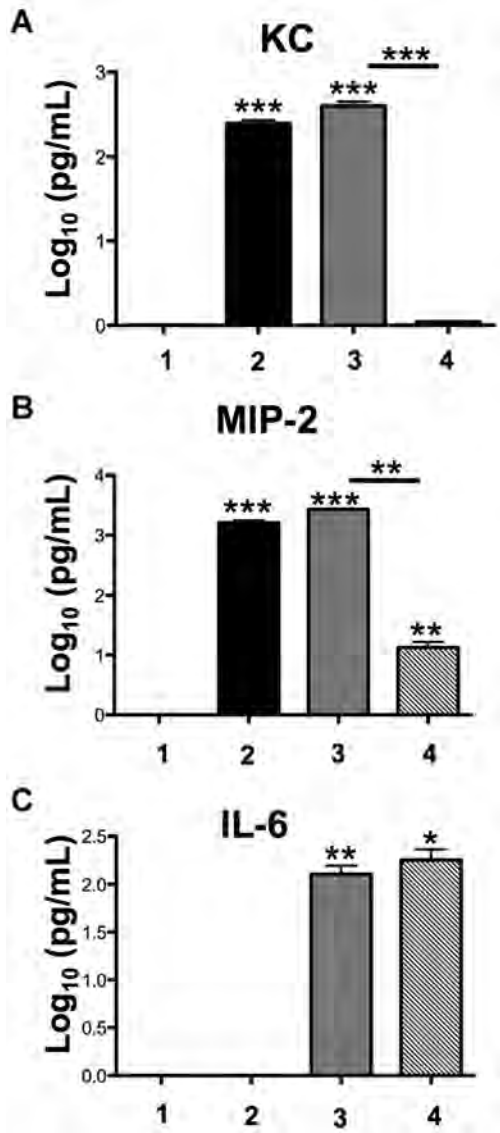

Fig. 5. Inflammatory response of bone remodeling unit in the presence of cancer cells. After MC3T3-E1 were cultured for 2 months, non-adherent bone marrow cells from dsRED mice enriched for pre-osteoclasts were added. Cultures were supplemented with RANKL (50 ng/ml) and MCSF (100 ng/ml) for 3 weeks (osteoblasts plus osteoclasts). Metastatic breast cancer cells, MDA-MB-231-GFP, were added to the osteoblast–osteoclast co-culture to create a tri-culture system as described in the methods. At the end of culture periods, supernatants were collected and assayed by ELISA for MIP-2 (mouse homologue of human IL-8) (A), KC (mouse homologue of human GRO-α) (B), and IL-6 (C). Sample size, n = 3. Unless indicated with a bar, statistical significance is in relation to cultures with only osteoblasts. 1 = osteoblasts, 2 = osteoblasts + osteoclasts, 3 = osteoblasts + osteoclasts + breast cancer cells, 4 = osteoblasts + breast cancer cells.

focus of recent investigation for this reason (Weaver et al., 1995; Nelson and Bissell, 2005). Surrogates for bone tissue are, however, quite challenging to construct (Kuperwasser et al., 2005). Models based on excised bone (Nemeth et al., 1999) are not only technically challenging but also difficult to interface with modern microscopic methods of investigation.

We implemented a specialized culture system (Supplementary Fig. 1) that permits growth of a non-vascularized, multiple-cell-layer osteoblastic tissue from isolated human and murine osteoblasts (Dhurjati et al., 2006, 2008; Krishnan et al., 2010). This approach permits phenotypic maturation of pre-osteoblasts through successive stages of proliferation, terminal differentiation, and mineralization into osteocyte-like cells embedded in a thick collagenous ECM over many months of continuous culture with no evidence of tissue necrosis. Temporal progression of

phenotype markers such as osteocalcin, osteonectin, type I collagen, MMP-13, and E1 all followed expectations of the classical stages of bone development (Krishnan et al., 2010).

Osteoclasts were derived from mouse bone marrow by culturing the non-adherent cells with RANKL and MCSF supplementation. The cells fused to form multinucleated osteoclasts (Fig. 1) that were capable of resorption when plated on dentine slices (data not shown). The co-culture of osteoblasts and osteoclasts is not a unique concept. Hattner et al. (1965) pioneered this concept, and it was further established by groups such as Suda, Vacanti, etc. (Jimi et al., 1996; Nakagawa et al., 2004). Similarly, in our system, extracted bone-marrow cells were enriched for pre-osteoclasts but were not further purified to eliminate other cell types of bone marrow such as endothelial cells, osteoblasts, fibroblasts, etc. This mixed population of cells simulated a physiologically relevant system. In addition to the activation of functional osteoclasts by osteoblasts through a cell–cell contact (Jimi et al., 1996), the putative cytokines and growth factors of the bone microenvironment presumably also stimulate osteoclastogenesis.

A major advantage of the 3D culture system used in this work is the development and maturation of a thick cell-derived collagenous matrix. It has been shown that the interaction of cells with reconstituted collagen layers or with Matrigel is fundamentally different than interaction with authentic cell-produced matrix (Sabeh et al., 2009; Lutter et al., 2010). In the 3D culture system used in this work, we observed the matrix degradation of an osteoblast-derived ECM by osteoclasts. The osteoclasts stained positive for TRAP and formed characteristic actin rings.

Achieving a balance between the matrix resorption and deposition requires the recruitment of fresh pre-osteoblasts. In the culture system used in this study, osteoblasts had terminally differentiated into mature osteoblasts engulfed in mineralized matrix (Krishnan et al., 2010) and were no longer proliferating. Therefore, we inoculated fresh pre-osteoblast MC3T3-E1 cells to refill the resorption pits created by the osteoclasts. To our knowledge this is the first report of an in vitro culture system that simulates bone remodeling.

Introduction of MDA-MB-231 metastatic breast cancer cells into the osteoblast/osteoclast co-culture created a tri-culture system consisting of the major cellular participants in the vicious cycle of metastatic cancer in bone. According to this paradigm, cancer cells secrete factors such as PTHrP that activate osteoclasts through intermediary stimulation of osteoblasts. Osteoblasts increase production of RANKL, which stimulates pre-osteoclasts to differentiate into mature, multinucleated osteoclasts that actively resorb bone. As the tissue is degraded by mature osteoclasts, various growth factors such as TGF-β are released that further stimulate osteoclastogenesis, thus amplifying and perpetuating a bone-degrading spiral of events (Guise and Chirgwin, 2003).

The vicious cycle is short-circuited in the absence of any one of the three participating cell types. Co-culture of osteoclasts with osteoblastic tissue results in resorption of mineralized tissue. Co-culture of metastatic breast cancer cells with osteoblastic tissue is more complex but also leads to destruction of mineralized tissue (Dhurjati et al., 2008; Krishnan et al., 2011). In particular, we have observed that breast cancer cells sequentially attach to osteoblastic tissue, proliferate, and form cell columns that penetrate the tissue over a 3 day co-culture interval in the absence of osteoclasts. Cell columns further organize into rows that are strikingly similar to the single cell files described for infiltrating lobular or metaplastic breast carcinomas (Page et al., 1987; Friedl and Wolf, 2003, 2008) and bone metastases (Mastro and Vogler, 2009). Decreases in secreted osteocalcin and soluble collagen accompanied by an increase in the inflammatory cytokine IL-6 were all concomitant with these morphological changes.

A different course of events was observed when the vicious cycle was enabled by tri-culture of osteoblastic tissue with osteoclasts and cancer cells. The migration of cancer cell to osteoclasts, and the formation of osteoclast and breast cancer cells into an aggregate were visual testimony of the three-way interaction among the primary cell participants of the vicious cycle. Mundy et al. (1981) reported that human tumor cells migrate unidirectionally in response to collagen and collagen derived fragments. The authors suggested that once breast cancer cells colonize the bone marrow, they are attracted to bone surfaces by the products of resorbing bone and subsequently proliferate by destroying bone via osteoclast stimulation (Yoneda et al., 1994; Body et al., 2006). We have shown that the osteoblasts become engulfed in a thick, native, cell-made ECM (Krishnan et al., 2010) providing a relevant model to study the interactions of osteoclasts and breast cancer cells. We observed a loss of type I collagen (as evidenced by a rise in C-telopeptide) in the presence of osteoclasts. Furthermore, addition of breast cancer cells resulted in the migration and penetration of cancer colonies through the layers of osteoblastic tissue to the substratum. Even though there was a visual reduction of collagen protein, we did not observe an increase in C-telopeptide levels in the presence of cancer cells. We speculate that the presence of cancer cells does not result in C-telopeptide generation but collagen breakdown through a phagocytic pathway possibly mediated through MT1-MMP. Aggressive breast cancer cells such as MDA-MB-231 cells have been shown to cleave collagen in $^{1}/_{4}$ or $^{3}/_{4}$ fragments through MT1-MMP activity (Lee et al., 2007). There was a significant increase in the number of TRAP positive osteoclasts and a subsequent increase in TRAP gene expression in the presence of breast cancer cells indicating that the presence of cancer cells promotes osteoclastogenesis from pre-osteoclasts.

Studies of the cancer colonization of bone have been primarily focused on the contribution of osteoclasts to the vicious cycle. Consequently, the majority of drugs in clinic have been focused on targeting the osteoclast activity as a means to stop osteolytic lesions. Despite osteoclast inhibition, bone is not completely repaired or regenerated in breast cancer patients with bone metastases, suggesting an important role for osteoblasts in the progression of disease. There is evidence from clinical and animal studies that bone loss in osteolytic metastasis is partly due to the failure of the osteoblasts to produce the osteoid for bone matrix (Stewart et al., 1982; Sasaki et al., 1995; Mercer et al., 2004). Similarly, administration of bisphosphonates to humans with osteolytic metastasis slows lesion progression but does not bring about healing (Lipton, 2000). Also, in vitro studies have shown that metastatic breast cancer cells increase apoptosis of osteoblasts, suppress osteoblast differentiation and induce an osteoblast inflammatory stress response (Mastro et al., 2004; Mercer et al., 2004). We have previously shown that metastatic breast cancer cells suppress the adhesion and differentiation of osteoblasts (Mercer et al., 2004). Similarly, in the bioreactor, the levels of osteocalcin expression were downregulated not only in the presence of osteoclasts but also with the addition of cancer cells demonstrating an important role for osteoblasts in this tri-culture interaction. We have also previously reported changes in inflammatory cytokines (MIP-2, KC, and IL-6) in vitro and in the bone microenvironment of athymic mice injected (intracardiac) with MDA-MB-231-GFP cells (Kinder et al., 2008; Bussard et al., 2010; Sosnoski et al., 2012). We also observed changes in these inflammatory cytokines in the bioreactor. MIP-2, an IL-8 human analogue, and inflammatory cytokine IL-6 are known to upregulate osteoclasts independent of RANKL pathway. We observed a threefold increase in MIP-2

with osteoclasts and the levels remained the same in the presence of cancer cells. However, there was no increase in levels of IL-6 with osteoclasts alone but a significant increase in the presence of breast cancer cells. Recent evidence from Sethi et al. (2011), suggests that the Notch ligand Jagged 1 plays an important role in the outgrowth of breast cancer cells to bone. They provide experimental and clinical evidence for IL-6 as the downstream target of the Jagged1-Notch pathway. Their data reinforce the vicious cycle model and a role for IL-6 as a pro-proliferative marker that propagates this cycle. In multiple myeloma, a cancer type that also targets bone as a secondary organ, it has been shown that osteoclasts enhance the growth and survival of multiple myeloma cells through the production of IL-6 (Abe et al., 2004). We speculate that a similar mechanism exists in the interaction between breast cancer cells and osteoclasts. The production of IL-6 concomitant with breast cancer and osteoclast cell–cell contact promotes proliferation of cancer cells and degradation of osteoblastic tissue. Our results provide evidence at both morphological and gene/protein levels that breast cancer cells degrade osteoblastic tissue via osteoclast stimulation in a 3D in vitro system comprised of tissue, resorbing osteoclasts, and metastatic breast cancer cells. Although, the phenomenon of breast cancer cell manipulation of the bone microenvironment is well accepted, there are no in vitro models to study the basic interactions of the three cell types. We propose a novel in vitro model that can accommodate the key cell types of the vicious cycle of bone metastases. Future studies will focus on understanding the mechanism behind interaction of breast cancer cells with the bioreactor-generated bone tissue. We will extrapolate this model to human-derived 3D osteoblast tissue to study interactions with other bone-metastatic cancers (e.g., osteoblastic prostate cancer cells or osteolytic multiple myeloma cells) to determine if human cancer colonization of human bone microenvironment parallels pathogenesis in vivo. The ability to directly observe and manipulate bone remodeling processes otherwise obscured by the inaccessibility of the marrow cavity will greatly improve fundamental understanding of osteobiology and osteopathologies involving bone remodeling.

Although the 3D system is a highly-simplified model of the marrow microenvironment lacking nerves, blood flow, adipocytes, etc. that undoubtedly play an important role in bone physiology, we contend that the combination of osteoblastic tissue, osteoclasts, and breast cancer cells display critical features of cancer metastases in bone. We anticipate that the bone-remodeling and vicious cycle mimics reported in this study will reveal subtle differences in the way various cancers (breast, lung, myeloma, prostate) engage the vicious cycle. These in vitro models may also resolve key differences between lytic and blastic manifestations of cancer in bone paving the way for accelerated development of novel therapeutic interventions.

Acknowledgment

We thank AMGEN®, Thousand Oaks, CA for the gift of recombinant RANKL, and the Microscopy and Cytometry Facility of the Huck Institutes of the Life Sciences.

Literature Cited

Abe M, Hiura K, Wilde J, Shioyasono A, Moriyama K, Hashimoto T, Kido S, Oshima T, Shibata H, Ozaki S. 2004. Osteoclasts enhance myeloma cell growth and survival via cell–cell contact: A vicious cycle between bone destruction and myeloma expansion. Blood 104:2484.

Bischoff DS, Zhu JH, Makhijani NS, Yamaguchi DT. 2005. KC chemokine expression by TGF-beta in C3H10T1/2 cells induced towards osteoblasts. Biochemical and biophysical research communications 326:364–370.

Body JJ, Facon T, Coleman RE, Lipton A, Geurs F, Fan M, Holloway D, Peterson MC, Bekker PJ. 2006. A study of the biological receptor activator of nuclear factor-kappaB ligand inhibitor, denosumab, in patients with multiple myeloma or bone metastases from breast cancer. Clin Cancer Res 12:1221–1228.

Bussard KM, Venzon DJ, Mastro AM. 2010. Osteoblasts are a major source of inflammatory cytokines in the tumor microenvironment of bone metastatic breast cancer. J Cell Biochem 111:1138–1148.

Curtin P, Youm H, Salih E. 2012. Three-dimensional cancer-bone metastasis model using ex-vivo co-cultures of live calvarial bones and cancer cells. Biomaterials 33:1065–1078.

Dhurjati R, Liu X, Gay CV, Mastro AM, Vogler EA. 2006. Extended-term culture of bone cells in a compartmentalized bioreactor. Tissue Eng 12:3045–3054.

Dhurjati R, Krishnan V, Shuman LA, Mastro AM, Vogler EA. 2008. Metastatic breast cancer cells colonize and degrade three-dimensional osteoblastic tissue in vitro. Clin Exp Metastasis 25:741–752.

Friedl P, Wolf K. 2003. Tumour-cell invasion and migration: Diversity and escape mechanisms. Nat Rev Cancer 3:362–374.

Friedl P, Wolf K. 2008. Tube travel: The role of proteases in individual and collective cancer cell invasion. Cancer Res 68:7247–7249.

Gabbert H. 1985. Mechanisms of tumor invasion: Evidence from in vivo observations. Cancer Metastasis Rev 4:293–309.

Gahwiler BH, Capogna M, Debanne D, McKinney RA, Thompson SM. 1997. Organotypic slice cultures: A technique has come of age. Trends Neurosci 20:471–477.

Griffith LG, Naughton G. 2002. Tissue engineering-current challenges and expanding opportunities. Science 295:1009–1014.

Guise TA, Chirgwin JM. 2003. Transforming growth factor-beta in osteolytic breast cancer bone metastases. Clin Ortho Rel Res 4155:532–538.

Guise TA, Mundy GR. 1998. Cancer and bone. Endocr Rev 19:18–54.

Hattner R, Epker BN, Frost HM. 1965. Suggested sequential mode of control of changes in cell behaviour in adult bone remodelling. Nature 206:489–490.

Hicks KO, Pruijn FB, Secomb TW, Hay MP, Hsu R, Brown JM, Denny WA, Dewhirst MW, Wilson WR. 2006. Use of three-dimensional tissue cultures to model extravascular transport and predict in vivo activity of hypoxia-targeted anticancer drugs. J Natl Cancer Inst 98:1118.

Jimi E, Nakamura I, Amano H, Taguchi Y, Tsurukai T, Tamura M, Takahashi N, Suda T. 1996. Osteoclast function is activated by osteoblastic cells through a mechanism involving cell-to-cell contact. Endocrinology 137:2187–2190.

Kim JB. 2005. Three-dimensional tissue culture models in cancer biology. Semin Cancer Biol 15:365–377.

Kinder M, Chislock E, Bussard KM, Shuman L, Mastro AM. 2008. Metastatic breast cancer induces an osteoblast inflammatory response. Exp Cell Res 314:173–183.

Krishnan V, Dhurjati R, Vogler EA, Mastro AM. 2010. Osteogenesis in vitro: From pre-osteoblasts to osteocytes. In Vitro Cell Dev Biol Anim 46:28–35.

Krishnan V, Shuman LA, Sosnoski DM, Dhurjati R, Vogler EA, Mastro AM. 2011. Dynamic interaction between breast cancer cells and osteoblastic tissue: Comparison of Two and Three dimensional cultures. J Cell Physiol 226:2150–2158.

Kuperwasser C, Dessain S, Bierbaum BE, Garnet D, Sperandio K, Gauvin GP, Naber SP, Weinberg RA, Rosenblatt M. 2005. A mouse model of human breast cancer metastasis to human bone. Cancer Res 65:6130–6138.

Landis SH, Murray T, Bolden S, Wingo PA. 1999. Cancer statistics. CA Cancer J Clin 49: 8–31.

Lee H, Sodek KL, Hwang Q, Brown TJ, Ringuette M, Sodek J. 2007. Phagocytosis of collagen by fibroblasts and invasive cancer cells is mediated by MT1-MMP. Biochem Soc Trans 35:704.

Liotta LA, Hart IR. 1982. Tumor invasion and metastasis: Leiden: Martinus Nijhoff Publishers/ Brill Academic Publi.

Lipton A. 2000. Bisphosphonates and breast carcinoma. Cancer 88:3033–3037.

Logothetis CJ, Lin SH. 2005. Osteoblasts in prostate cancer metastasis to bone. Nat Rev Cancer 5:21–28.

Lutter AH, Hempel U, Wolf Brandstetter C, Garbe AI, Goettsch C, Hofbauer LC, Jessberger R, Dieter P. 2010. A novel resorption assay for osteoclast functionality based on an osteoblast derived native extracellular matrix. J Cell Biochem 109:1025–1032.

Mastro AM, Vogler EA. 2009. A three-dimensional osteogenic tissue model for the study of metastatic tumor cell interactions with bone. Cancer Res 69:4097–4100.

Mastro AM, Gay CV, Welch DR. 2003. The skeleton as a unique environment for breast cancer cells. Clin Exp Metastasis 20:275–284.

Mastro AM, Gay CV, Welch DR, Donahue HJ, Jewell J, Mercer R, DiGirolamo D, Chislock EM, Guttridge K. 2004. Breast cancer cells induce osteoblast apoptosis: A possible contributor to bone degradation. J Cell Biochem 91:265–276.

Mercer RR, Miyasaka C, Mastro AM. 2004. Metastatic breast cancer cells suppress osteoblast adhesion and differentiation. Clin Exp Metastasis 21:427–435.

Mundy GR, Demartino S, Rowe DW. 1981. Collagen and collagen-derived fragments are chemotactic for tumor cells. J Clin Invest 68:1102.

Nakagawa K, Abukawa H, Shin MY, Terai H, Troulis MJ, Vacanti JP. 2004. Osteoclastogenesis on tissue-engineered bone. Tissue Eng 10:93–100.

Nelson CM, Bissell MJ. 2005. Modeling dynamic reciprocity: Engineering three-dimensional culture models of breast architecture, function, and neoplastic transformation. Semin Cancer Biol 15:342–352.

Nemeth JA, Harb JF, Barroso U, Jr., He Z, Grignon DJ, Cher ML. 1999. Severe combined immunodeficient-hu model of human prostate cancer metastasis to human bone. Cancer Res 59:1987–1993.

Nielsen OS, Munro AJ, Tannock IF. 1991. Bone metastases: Pathophysiology and management policy. J Clin Oncol 9:509–524.

Nordstrand A, Nilsson J, Tieva A, Wikstrom P, Lerner UH, Widmark A. 2009. Establishment and validation of an in vitro co-culture model to study the interactions between bone and prostate cancer cells. Clin Exp Metastasis 26:945–953.

Page DL, Anderson TJ. 1987. Diagnostic histopathology of the breast. Churchill Livingstone: Edinburgh, pp 219–222.

Papadimitropoulos A, Scherberich A, Guven S, Theilgaard N, Crooijmans HJ, Santini F, Scheffler K, Zallone A, Martin I. 2011. A 3D in vitro bone organ model using human progenitor cells. Eur Cells Mater 21:445–458;discussion 458.

Phadke PA, Mercer RR, Harms JF, Jia Y, Frost AR, Jewell JL, Bussard KM, Nelson S, Moore C, Kappes JC, Gay CV, Mastro AM, Welch DR. 2006. Kinetics of metastatic breast cancer cell trafficking in bone. Clin Cancer Res 12:1431–1440.

Rubens RD. 1998. Bone metastases—The clinical problem. Eur J Cancer 34:210–213.

Rubens RD, Mundy GR. 2000. Cancer and the skeleton. London: Martin Dunitz.

Sabeh F, Shimizu-Hirota R, Weiss SJ. 2009. Protease-dependent versus-independent cancer cell invasion programs: Three-dimensional amoeboid movement revisited. J Cell Biol 185:11.

Sakai T, Larsen M, Yamada KM. 2003. Fibronectin requirement in branching morphogenesis. Nature 423:876–881.
Sasaki A, Boyce BF, Story B, Wright KR, Chapman M, Boyce R, Mundy GR, Yoneda T. 1995. Bisphosphonate risedronate reduces metastatic human breast cancer burden in bone in nude mice. Cancer Res 55:3551.
Sethi N, Dai X, Winter CG, Kang Y. 2011. Tumor-derived JAGGED1 promotes osteolytic bone metastasis of breast cancer by engaging notch signaling in bone cells. Cancer Cell 19:192–205.
Smalley KSM, Lioni M, Herlyn M. 2006. Life ins't flat: Taking cancer biology to the next dimension. In Vitro Cell Dev Biol Anim 42:242–247.
Sosnoski DM, Krishnan V, Kraemer WJ, Dunn-Lewis C, Mastro AM. 2012. Changes in cytokines of the bone microenvironment during breast cancer metastasis. Int J Breast Cancer 2012:160265.
Stewart AF, Vignery A, Silverglate ANN, Ravin ND, LiVolsi V, Broadus AE, Baron R. 1982. Quantitative bone histomorphometry in humoral hypercalcemia of malignancy: Uncoupling of bone cell activity. J Clin Endocrinol Metabol 55:219.
Weaver VM, Howlett AR, Langton-Webster B, Petersen OW, Bissell MJ. 1995. The development of a functionally relevant cell culture model of progressive human breast cancer. Semin Cancer Biol 6:175–184.
Welch DR. 1997. Technical considerations for studying cancer metastasis in vivo. Clin Exp Metastasis 15:272–306.
Woodhouse EC, Chuaqui RF, Liotta LA. 1997. General mechanisms of metastasis. Cancer 80:1529–1537.
Yoneda T, Sasaki A, Mundy GR. 1994. Osteolytic bone metastasis in breast cancer. Breast Cancer Res Treat 32:73–84.

Supporting Information

Additional supporting information may be found in the online version of this article at the publisher's web-site.